

P-541



A PROPOSAL TO STUDY NEUTRAL CURRENT NEUTRINO AND ANTINEUTRINO INTERACTIONS

Submitted to the 1977 Fermilab Neutrino Workshop
April 21-22, 1977

B. Eisenstein, L. Holloway
University of Illinois at Urbana Champaign

A. L. Sessoms, C. Tao, R. Wilson
Harvard University

S. C. Wright
University of Chicago

SPOKESMAN:

A. L. Sessoms
High Energy Physics Laboratory
42 Oxford Street
Cambridge, Massachusetts 02138
617-495-5889
(FTS 830-5889)

63 pgs.

ABSTRACT

We propose to build a liquid argon/iron hadron calorimeter to be used in conjunction with the HPWF muon spectrometer to study the neutral current interactions of neutrinos at Fermilab. The device will have an energy resolution of $\sigma_{E_H} = 0.5/\sqrt{E_H}(\text{Gev})$, and the ability to measure the direction of the hadrons shower with an accuracy of $\sigma(\theta_H) = 0.004 + 0.6/E_H$ radians. We propose to carry out detailed studies of the cross sections as functions of $x = Q^2/2M_p\nu$, $y = \nu/E_\nu$ and W^2 , the invariant mass of the hadronic final state. We will also be alert to any anomalous production of muons associated with neutral current events. We propose to situate the calorimeter such that only neutrinos from K meson decays enter the target. This ensures that the neutrino energy is known to better than 10% and that large kinematic ranges in x and y are covered.

Table of Contents

Abstract

Table of Contents

I. Introduction

II. Physics Motivation

III. Apparatus

IV. The Beam and Event Rates

V. Comparison with CERN SPS

VI. Cost Estimate and Time Scale

VII. Summary

References

I. Introduction

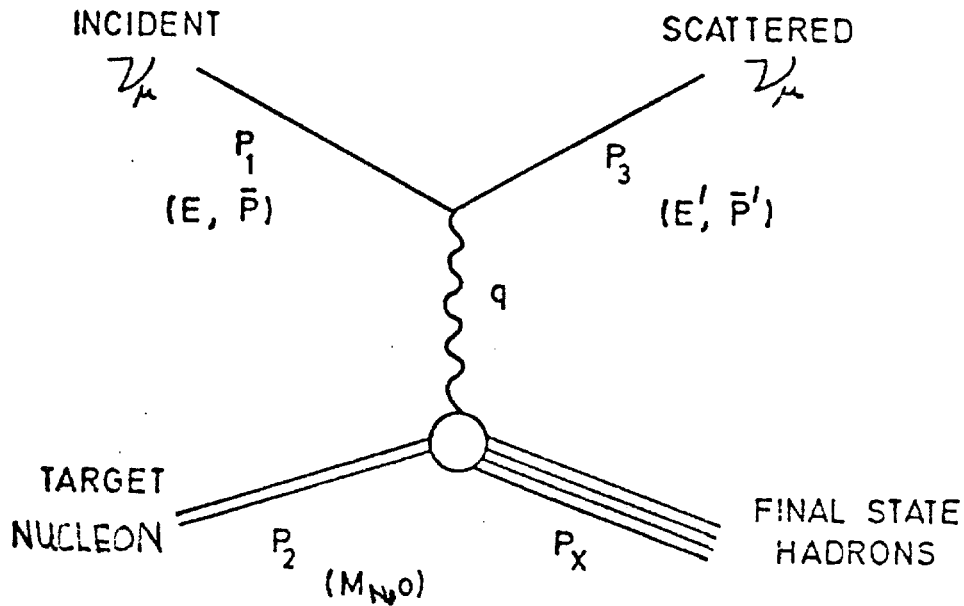
After four years of experimentation in neutrino physics at Fermilab it is clear that we have only scratched the surface of the wealth of information to be gained from this exciting field. Several anomalies exist in charge current interactions that point to new and very interesting phenomena such as new quarks.^{1,2} Experimentally, very little is known about neutral current interactions; it is reasonable to expect much excitement to be generated by careful and detailed studies.

The present data from neutrino experiments often lack statistical power and, in the case of neutral currents, also lack adequate knowledge of ν and Q^2 (or x and y), to allow detailed studies to be made. These limitations induce theorists to use the data much the way drunkards use lampposts (for support rather than illumination).³

New technological developments allow the construction of an apparatus which we believe compares favorably with present efforts at CERN in both capability and time scale for the study of neutrino induced neutral current interactions with the dichromatic beam presently under construction at Fermilab.⁴ We propose to build such a detector.

We first discuss the physics motivation behind such an endeavor. We then describe the proposed apparatus and compare it with existing experiments at the CERN SPS.

LOWEST ORDER FEYNMANN DIAGRAM FOR



$$q = P_1 - P_3$$

$$\mathcal{V} = q \cdot P_2 / M_P = E - E'$$

θ is the angle between \vec{p} and \vec{p}'

$$q^2 = -2EE' + 2\vec{p}\vec{p}' \cos \theta \leq 0$$

$$P_X^2 = (P_2 + q)^2 = M_N^2 + 2M_N \mathcal{V} + q^2$$

Since baryon number is conserved,

$$P_X^2 \geq M_N^2, \text{ which implies } -q^2 \leq 2M_N \mathcal{V}$$

A convenient and highly accurate expression is

$$-q^2 = 4EE' \sin^2 \theta/2$$

II. Physics Motivation

With the discovery of neutral current phenomena a few years ago we now face a situation similar to that encountered in the early days ($t \leq 1957$) of β -decay: we now must determine the nature of the effective Lagrangian governing neutral-current phenomena. The processes which have been observed include

$$\nu_{\mu} + N \rightarrow \nu_{\mu} + \text{hadrons}$$

$$\bar{\nu}_{\mu} + N \rightarrow \bar{\nu}_{\mu} + \text{hadrons}$$

$$\bar{\nu}_{\mu} + e^{-} \rightarrow \bar{\nu}_{\mu} + e^{-}$$

$$\bar{\nu}_{e} + e^{-} \rightarrow \bar{\nu}_{e} + e^{-}$$

A fairly general candidate effective Lagrangian for these reactions is³³

$$L_{\text{eff}} = \frac{G}{\sqrt{2}} \bar{\nu}_{\mu} \gamma^{\lambda} (1 - \gamma_5) \nu_{\mu} \left[\begin{array}{l} \epsilon_L(e) \bar{e} \gamma_{\lambda} (1 - \gamma_5) e \\ + \epsilon_R(e) \bar{e} \gamma_{\lambda} (1 + \gamma_5) e \\ + (e \leftrightarrow \mu) \\ + \epsilon_L(u) \sum_{i=1}^3 \bar{u}_i \gamma_{\lambda} (1 - \gamma_5) u_i \\ + \epsilon_R(u) \sum_{i=1}^3 \bar{u}_i \gamma_{\lambda} (1 + \gamma_5) u_i \\ + (u \leftrightarrow d) \\ + (u \leftrightarrow s) \end{array} \right]$$

$$\begin{aligned}
 & \left[\begin{array}{l} + (u \leftrightarrow c) \\ + \dots \end{array} \right] \\
 + \frac{G}{\sqrt{2}} & \left[\begin{array}{l} \epsilon_{LL} (e, u) \bar{e} \gamma^\lambda (1 - \gamma_5) e \sum_{i=1}^3 \bar{u}_i \gamma_\lambda (1 - \gamma_5) u_i \\ + \epsilon_{RL} (e, u) \bar{e} \gamma^\lambda (1 + \gamma_5) e \sum_{i=1}^3 \bar{u}_i \gamma_\lambda (1 - \gamma_5) u_i \\ + \dots \end{array} \right]
 \end{aligned}$$

In constructing such a Lagrangian several vital assumptions are usually made.³³

These include:

(1) The neutrino emitted in ν -induced neutral current processes is the same type as the incident neutrino. This must include helicity: if neutral currents proceed through

$$\nu_{\mu L} + N \rightarrow \nu_{\mu R} + \text{hadrons}$$

this would imply the existence of a new degree of freedom, and concomitant scalar, pseudoscalar or tensor neutral current couplings.^{7,34}

(2) The nonexistence of off diagonal neutral current reactions, e.g. charm changing processes such as $\nu_\mu + u_i \rightarrow \nu_\mu + c_i$. While the absence of $\Delta S = 1$ neutral currents and the motivation for charm (GIM mechanism) suggest their absence, this is not an inevitability and should be tested.

(3) The correctness of the 4-fermion nonderivative coupling structure of the Lagrangian.

(4) The use of the singlet fractionally charged quark structure. One might be able to build a Pati-Salam-like scheme,^{35,36} with broken color degrees of freedom, which might look very different from the assumed Lagrangian.

These assumptions, and others can be tested in a high statistics high resolution neutral current experiment. These tests might include:

(1) Detailed studies of the x and y distributions of the neutral current cross section. Helicity flip with spin-zero exchange favors large-angle neutrino scattering; in the scaling limit this results in a y^2 distribution ($y = E_{\text{hadron}}/E_\nu$) for the inclusive cross section. The CITF group has studied this distribution and finds it relatively flat.⁸ If the neutral current is diagonal, as is usually assumed, then for the (S, P) case (and the pure V or pure A cases)

$$d\sigma(\nu \rightarrow \nu) = d\sigma(\bar{\nu} \rightarrow \bar{\nu});$$

we know this is not true.⁷ The behavior of these cross sections as a function of $x = Q^2/2m_p \nu$ and y will give information on the detailed structure of the neutral current and possibly allow a statement on combinations of S, P, T and V, A interactions to be made. Combinations of this sort are not ruled out by any data at present.

(2) Searches for evidence of narrow resonances in the invariant cross sections as a function of W^2 , the invariant mass of the hadronic system. Any narrow structure would indicate the excitation of new degrees of freedom. As

in the production of charm by charged currents, the existence of single "wrong" signed muons would signal the production of new (or old, like charmed) particles and so off diagonal terms.

(3) Measurements of the E_ν and Q^2 dependence of neutral current processes would indicate whether any non-derivative terms manifest themselves at high energies.³²

(4) It has recently been pointed³⁵ out that a clean test of the hypothesis that hadronic gauge color is physical (quarks are integrally charged) and that it is excited at relatively low energies ($E_{\nu,\bar{\nu}} \gtrsim 50$ GeV) is possible through accurate measurements of neutral current cross sections at high energies. It is noted that within this theory one expects to see significant rises in the neutral current parameters due to color excitation; σ_{NC}^ν should rise 40 to 45%, $\sigma_{NC}^{\bar{\nu}}$ 60 to 65%, $R_\nu \equiv \sigma_{NC}^\nu / \sigma_{CC}^\nu$ should rise about 20%, and R about 10%. The authors also remark that, unlike the situation with charged current scattering where either new flavor or color excitation may lead to a rise in these parameters, rises in neutral current parameters cannot easily be attributed to new flavor thresholds within the $SU(2)_W \times U(1)$ gauge structure. They suggest that rises of this sort would point unambiguously to physical color excitation.

Charged Currents

Since the charged current neutrino cross section will be known quite well by 1979 we can use these events to directly measure the flux of neutrinos and antineutrinos incident on the detector. This will also allow careful comparisons of $d\sigma/dx$ and $d\sigma/dxy$ for charged and neutral currents to be made with little or no inherent systematic differences between the two data sets.

Comparisons of the production of multimuon final states for charged and neutral currents are also easily made.

We also note that because of our knowledge of the hadron direction we have 3 constraint fits for all charged current interactions; we only miss the mass of the hadronic system. Giving up E_ν we have a 2 constraint fit. This power will allow us to check any interesting details that may have been seen or hinted at in other experiments; we have a high resolution probe of the details of charged current processes.

In all of the above studies the important variables are $x = Q^2/2m_p \nu$, and $y = \nu/E_\nu$. It is essential to have the best possible resolution in x and y and the largest range, especially in y , if we are to make important statements about the structure of the weak interaction. It is here one decides to sacrifice statistics for accuracy and a large kinematic acceptance in these variables.

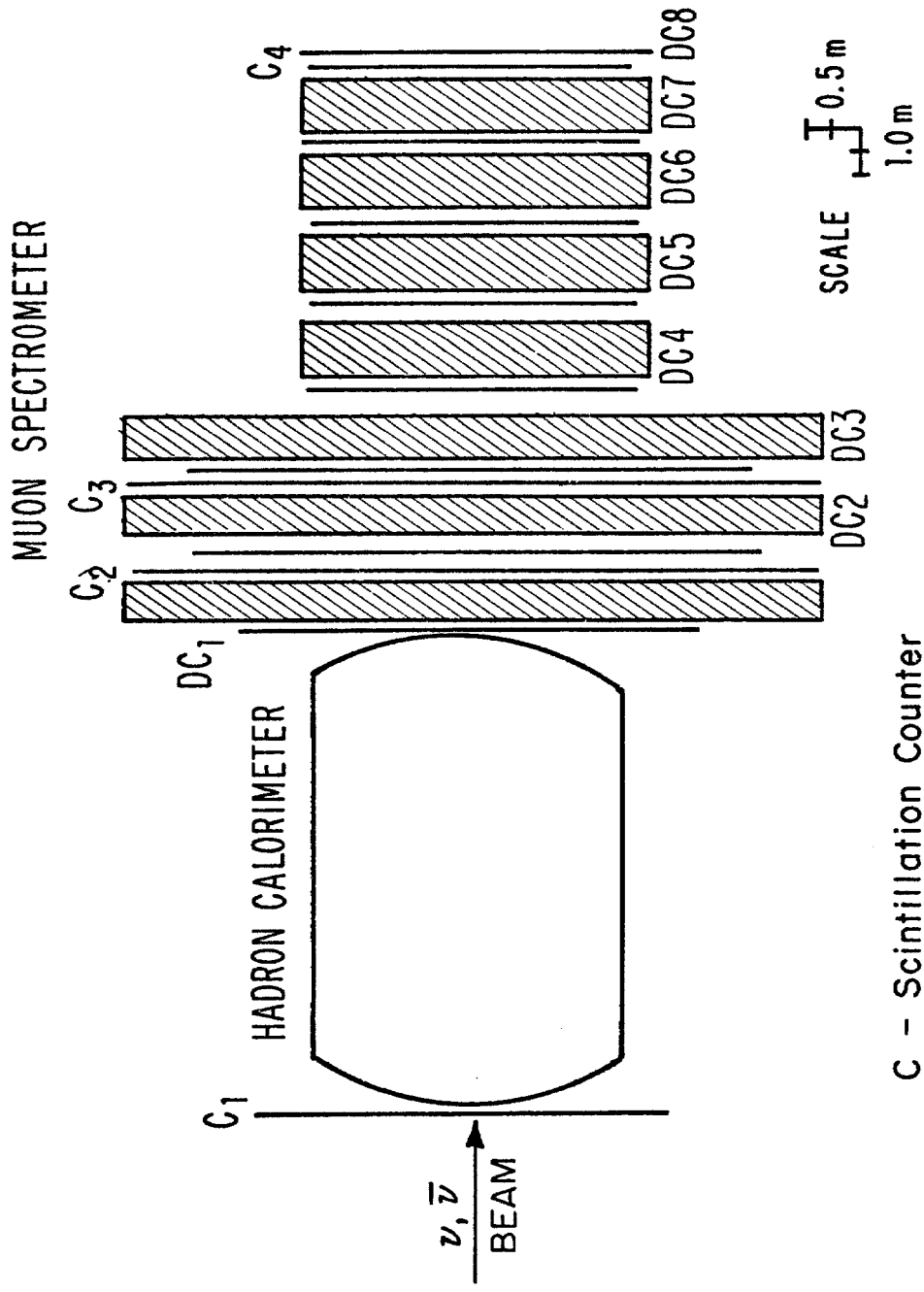
III. Apparatus

We propose to build a large iron/liquid argon calorimeter that would be used in conjunction with the Harvard-Penn-Wisconsin-Fermilab muon spectrometer with its spark chambers replaced by drift chambers. A drawing of the proposed experimental setup is given in Figure 1. An engineering drawing of the proposed calorimeter is given in Figure 2. Details are given in Table 1.

A. Calorimeter

The proposed calorimeter is contained in a dewar approximately 14 meters long and 4.7 meters in diameter. The calorimeter plates are steel, 1.5 mm thick and 3.6 m \times 3.6 m square. Each "plate" is made up of 4 sections 3.6 m \times 0.75 m \times 1.5 mm; there are 1400 such plates. These plates are divided into 140 sections of 10 plates, every two plates of which are followed by a set of 2 planes of steel strips 2 cm wide and 1.5 mm thick, 3.6 meters long. The strips are oriented in the x and y directions. This permits a measurement of the direction of the shower, as well as its energy, as will be discussed later.

A study incorporating these ideas is given in Figure 2. Several engineering studies of different configurations have been made. The final size of the calorimeter is determined by the divergence of the neutrino beam which in turn is determined by the spot size of the primary proton beam at the target. To come up with a size of 3 m \times 3 m for the fiducial area of the plates we assume a spot size of roughly 1 mm, which gives a pion and k-meson divergence of 0.22 mrad. This means that at 1 mrad the



C - Scintillation Counter
DC - Drift Chamber

FIG. 1 EXPERIMENTAL ARRANGEMENT

Table 1Target Calorimeter

Active Dimensions	$3.6 \times 3.6 \text{ m}^2$
Length	12.5 m
Sampling Step	1.5 mm iron (1.18 gm/cm^2)
Sampling Counter (Energy)	Liquid argon, 2 mm thick, iron plates $3.6 \times 3.6 \text{ m}^2$
Sampling Counter (Angle)	Liquid argon, 3 mm thick, iron plates $3.6 \text{ m} \times 0.02 \text{ m}$ x and y, every 16 mm
Modularity	140 modules of $10, 3.6 \times 3.6 \text{ m}^2 \times 1.5 \text{ mm}$ plates and 5 sets of $3.6 \times 0.02 \text{ m}^2 \times 1.5 \text{ mm}$ x and y strips
Total Quantities	Target weight 327 tons Target thickness 4089 gms/cm^2 Total weight 788 tons 30,000 channels of electronics
Average Quantities	Density $\rho = 4.17 \text{ gms/cm}^3$ Radiation length: 8.75 cm Interaction length: 34.7 cm
Performance	<u>Vertex Resolution</u> $\sigma = 0.6 \text{ cm}$ <u>Shower Direction</u> $\sigma(\theta_H) = 0.004 + \frac{0.6(\text{GeV})}{E_H}$ or $\pm 10 \text{ mrad}$ at 100 GeV <u>Hadron Energy Resolution</u> $\frac{\sigma(E_H)}{E_H} = \frac{0.5}{\sqrt{E(H)}}$

divergence of the neutrino beam is almost completely determined by the decay kinematics of pion and K-meson decay.

We can make use of this effect to almost completely eliminate the pion neutrinos from the detector and only accept kaon neutrinos, which will allow the energy to be known to roughly $\pm 9\%$. This accuracy depends on the angular divergence of the charged particle beam and its momentum resolution, assumed here to be $\pm 9\%$. This momentum spread completely dominates the knowledge of E_ν .

If the detector is large enough to detect neutrinos at ± 1 mrad, centered at about 2 mrad, a large fraction of the kaon neutrino spectrum is covered in a single exposure. This is discussed further in the section on the beam.

Dewar

The dewar design follows standard cryogenic practice. Its construction will be double walled steel with the space filled with superinsulation and evacuated. The supports will be low heat loss columns of the type used at Fermilab for superconducting magnets.¹⁷ The heat loss per column should be roughly 100 milliwatts.

Both ends of the dewar will be removeable to facilitate construction of the calorimeter, which will proceed from the middle out in both directions. The support columns have air pads of the type used on large spectrometer magnets at Cornell¹⁹ at the base. This will allow the calorimeter to be moved into place after being assembled in an open region.

The cooling will be carried out with liquid nitrogen through heat exchange coils inside the dewar. A reservoir will be used to store the liquid argon between fills and also to serve as a continuous supply during operation. The

purity of the liquid argon will be continuously monitored and purification initiated when necessary; the indications are²⁰ that purification will not be required very often. Figure 3 illustrates the liquid argon monitoring and purification system.

We expect the total heat loss from the calorimeter to be less than 4 watts.

The choice of the size and composition of the calorimeter were dictated by the desire for full shower containment and the best possible energy resolution coupled with a large acceptance, as discussed above, and good measurement of the direction of the shower. We discuss each in turn.

Shower Containment

Measurements of hadron shower development at 100 GeV in an iron-plastic scintillator calorimeter has recently been made by a CERN group.³¹ The data show the somewhat surprising fact that the showers do not spread out radially as they develop horizontally; the shower is cigar shaped. This indicates that, in iron, only 30 cm need be allowed radially to totally contain the shower.³¹

A group at Oak Ridge²¹ has calculated shower development in iron-liquid argon, iron-plastic scintillator, and uranium-liquid argon for a variety of hadron energies. Indications are that in order to contain at least 99% of a hadron shower greater than 6 collision lengths (3 absorption lengths) horizontally with respect to the axis of the shower development must be allowed. Measurements by two CERN groups^{20,31} and by CITF²² and HPWF²² verify these numbers. This is illustrated in Figure 4 taken from reference 20.

We have allowed 6 collision lengths horizontally in order to insure that we have essentially complete containment. We have also allowed 5 collision

ARGON HANDLING & PURIFICATION SYSTEM

- ☒ MANUAL VALVE
- ☒ SAFETY VALVE
- ☒ SOLENOID VALVE
- ⌚ HEAT EXCHANGER
- ⊕ MIN / MAX MANOMETER

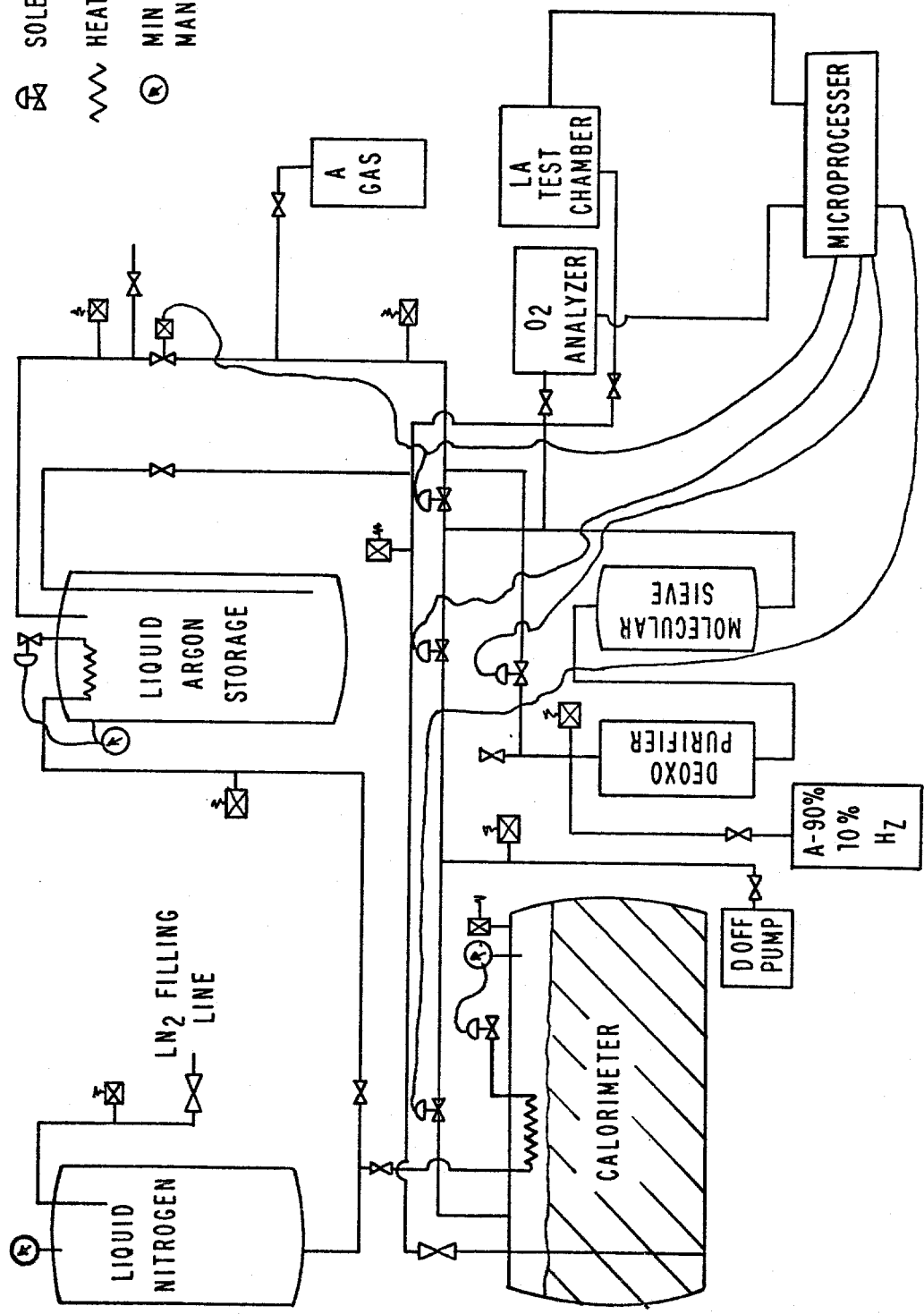


FIGURE 3

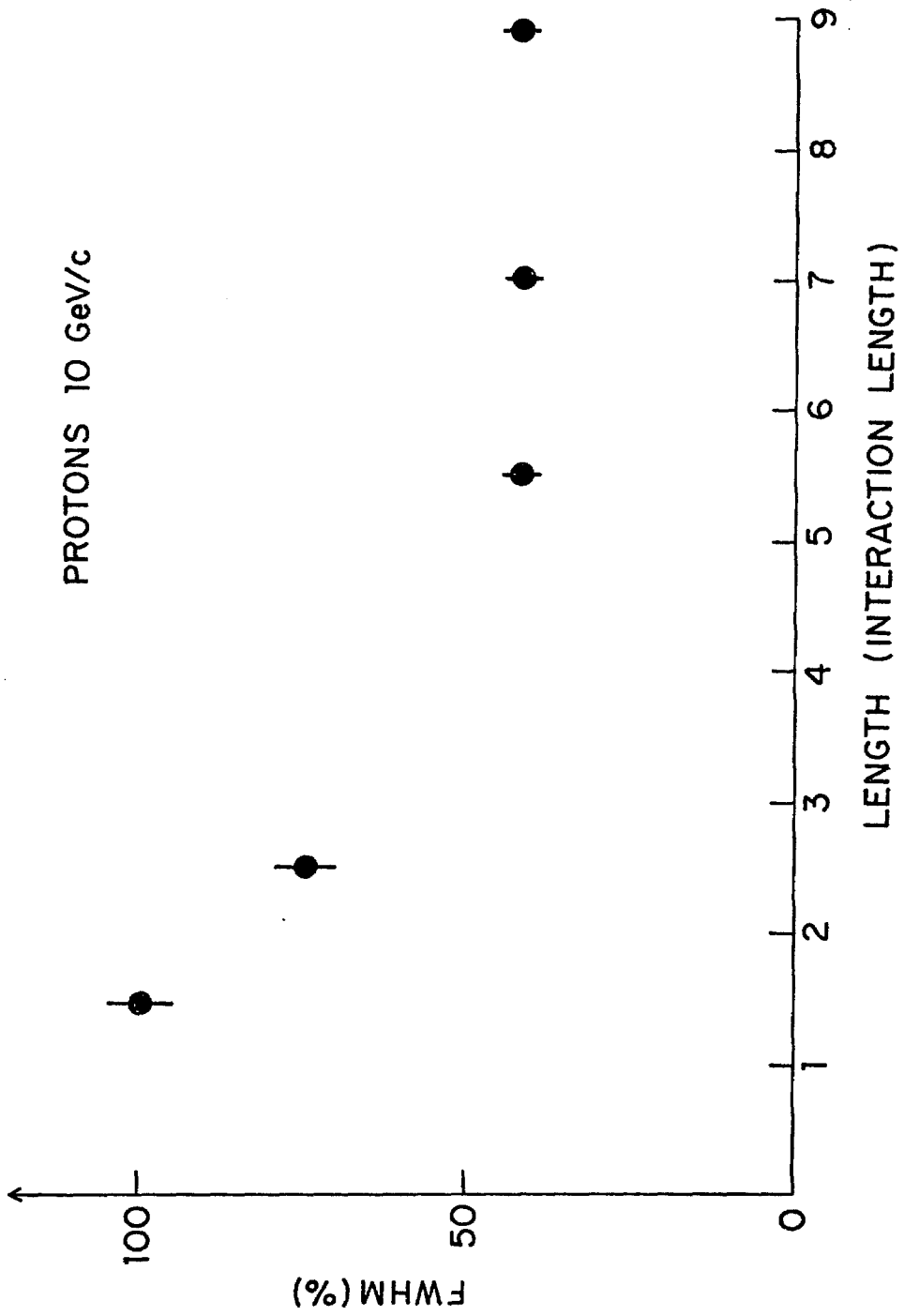


FIGURE 4

lengths in front of our fiducial volume to filter out hadrons in the beam.

Energy Resolution

Here we follow almost verbatim the discussion in reference 20.

Factors Which Limit the Resolution in Hadron Calorimeters

It may be useful to summarize briefly the processes which occur in a hadronic cascade. The hadron interacts with a nucleus after approximately one interaction length, generating typically several charged pions and several neutral pions, depending upon the incident energy, as well as a number of relativistic protons and a number of nuclear fragments. These last will be neutrons of energies of a few MeV and charged particles of very short range, including slow protons, deuterons, α -particles, and heavier fragments. The photons from neutral pions rapidly lead to electromagnetic showers which deposit all their energy by ionization of relativistic electrons. The charged pions and relativistic protons go about another nuclear interaction length and make further nuclear interactions which lead to the same kinds of particles in the final state. The nuclear fragments rarely interact again, but deposit their energy near the first interaction in the form of high ionization density tracks. The neutrons deposit their kinetic energy by elastic and inelastic collisions, and upon being captured by nuclei yield their binding energy of a few MeV in the form of photons, although this may happen at distances of many interaction lengths from the original source. Certain forms of energy are not visible in the absorber as ionization. These are: energy lost by neutrinos, mostly from pions at rest; high energy muons from decays which

have very long range; and that energy which is required to break up the nuclei, or nuclear binding energy. Most ionization detectors are also less than completely sensitive to particles of high ionization density, so that some of this ionization is effectively lost. In some absorbers it may be very difficult to retain all the energy of the neutrons. For example, in iron the interaction cross-section for neutrons of a few MeV energy is very small.

It is interesting to look at the results of the Oak Ridge Group²¹ on the form in which ionization is eventually deposited, as shown in Table 2. It can be seen that the most important forms in which energy is deposited are due to the electromagnetic cascades from π^0 's, as well as that due to slow particles. The fast pions deposit relatively little of the whole. It is also surprising what a large fraction of energy goes into nuclear binding energy.

A useful simple picture of the cascades is to consider them as being made up of two components: an electromagnetic shower component due to the neutral pions, and another component associated with the nuclear fragments. The division of energy between these shown in Table 2 is only true on the average, while individual events show a large fluctuation in the ratio of these two components because their contributions are determined largely by the nature of the very first interaction, where only a few particles are involved, particularly at low incident energies. The different response of a calorimeter to each of these two components proves to be the most important phenomenon affecting the performance of hadron calorimeters.

In the light of the above discussion, we may list those fluctuations which limit the resolution of hadron energy measurement.

- 1) *Fluctuations in the leakage of ionizing particles.* This can be reduced by making the absorber sufficiently large, but the range

Table 2

Average fractional energy deposition by particle type for 10 GeV proton interactions in an iron-argon calorimeter^{a)}

Type of energy deposition	Percent of total
Primary proton ionization	2.3
Secondary proton ionization	31.6
Secondary π^{\pm} ionization	8.2
μ^{\pm} ionization	0.05
Electromagnetic cascade	21.0
Z > 1 ionization	2.4
Residual nuclear excitation energy	3.7
Neutrons with energy > 10 MeV transported to a radius ≥ 2 interaction lengths	4.9
Neutrons with energy < 10 MeV	3.9
Nuclear binding energy plus neutrino energy	20.6

a) T.A. Gabriel and W. Schmidt, Calculated performance of iron-argon and iron-plastic calorimeters for incident hadrons with energies of 5 to 75 GeV, ORNL/TM-5105 (1975).

of high energy muons is such that they cannot possibly be contained. There is also a loss of particles out of the face of the absorber through which the incident particle enters, albedo. This can be eliminated if we reject those events where the interaction is in the first interaction length of the absorber. However, if we are not willing to accept substantial inefficiencies, this effect remains to limit the energy resolution.

- i) *Fluctuations in the leakage of non-ionizing particles.* Neutrinos will escape from any absorber. Hadrons are in principle retained, except for albedo, but in practice an absorber which is large enough to contain most hadrons still leaks neutrons of a few MeV, particularly when a material such as iron is used.
- iii) *Fluctuations in nuclear binding energy* necessary to disrupt the nuclei in the cascade. This energy is not directly detectable.
- iv) *Fluctuations in the saturation of the detector response* to particles of high ionization density. This saturation of response is present in almost every detector of ionizing radiation, but to different degrees. It can cause the effective loss of most of the energy corresponding to slow protons and heavier nuclear fragments.
- v) *Sampling fluctuations.* These are the fluctuations associated with the fact that in most calorimeters not all of the ionization is measured, but only periodically sampled. Even in those few detectors which use a homogeneously sensitive detector, some dead regions in the absorber are unavoidable and therefore may contribute a fluctuation of this type.

- vi) *Noise*. This includes effects of photon statistics in scintillation detectors, amplifier noise, and signal distortions due to slow neutrons from previous events or pile-up of events occurring within the time resolution of the detector.
- vii) *Fluctuations due to non-uniform response*. This effect would be absent in an ideal detector, but many calorimeters which have actually been built clearly suffered to some degree from this effect. We include here such effects as the non-uniform response across a given section of the detector, and different responses due to errors in calibration between different sections of a detector.

The CERN group²⁰ has concluded that, in a detector of sufficient size so that leakage of fast particles is not important, the resolution is dominated by nuclear fluctuations.

It is clear that the best way to compensate for these fluctuations is with U^{238} plates where one gains by fission amplification. However, measurements made at CERN³² indicate that, in order to get adequate angular resolution, it is necessary to sample radially along the shower at intervals of 1 radiation length; for uranium this is 3 mm! The resolution in the angle of the shower dominates the hadron energy resolution when applied to the uncertainty in $x = Q^2/m_p v$; this is illustrated in Figures 5 and 6.

We have found that iron (steel) allows a significantly better measurement of the angle, by almost a factor of 5, using a strip sampling width of 2 cm (~ 1 rad length). We lose only a factor of 2 or so in the energy resolution with iron over uranium. This is shown in Figure 7 where we plot energy resolution

$\frac{\sigma_x}{x}$ DUE TO ERROR IN HADRON ENERGY MEASUREMENT ($\equiv \sigma_n$)
FOR $E_\nu = 260$ Gev, $E_n = yE_\nu$

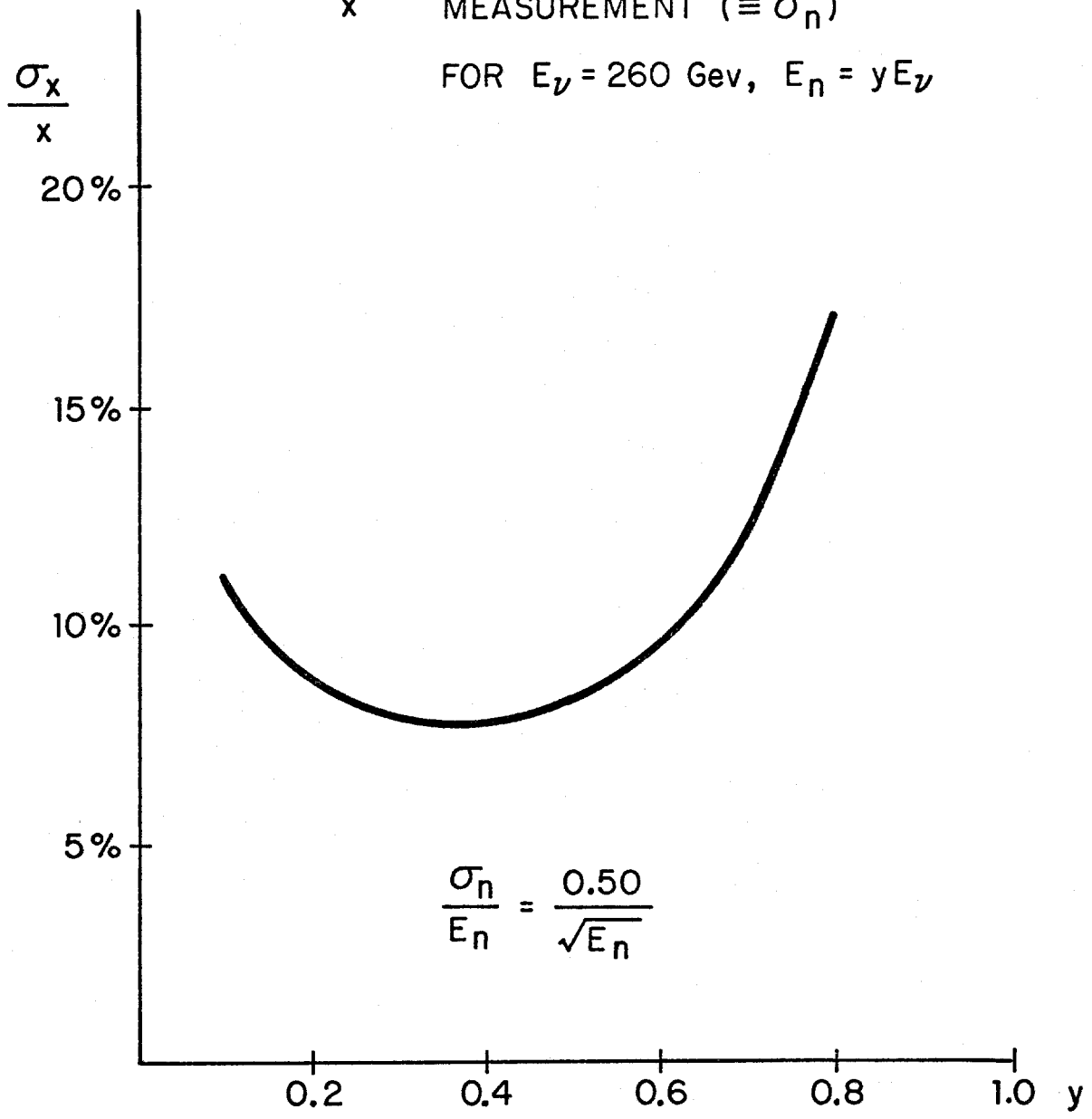


FIGURE 5

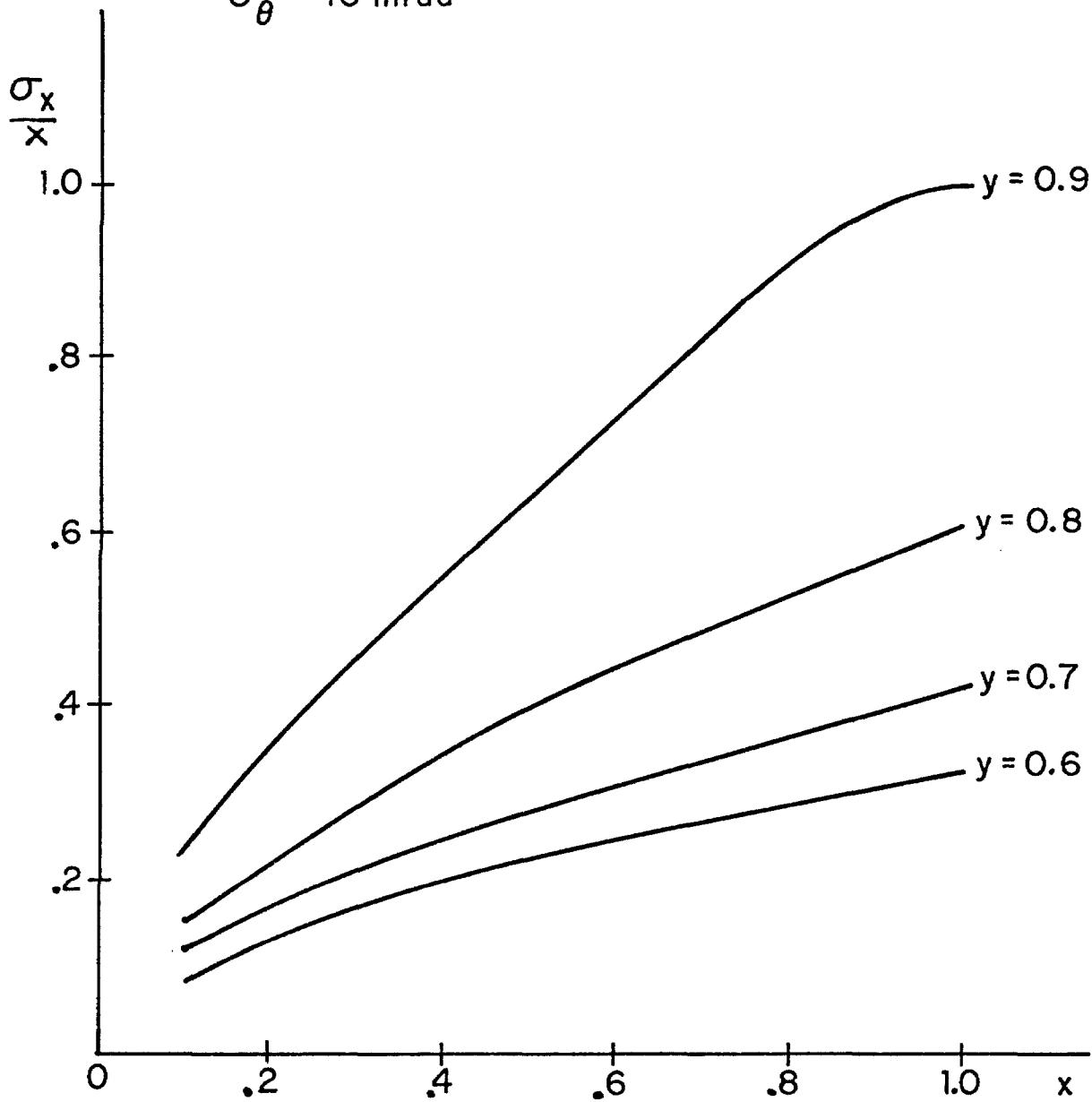
σ_x VS x FOR VARIOUS y ASSUMING $\sigma_\theta = 10$ mrad

FIGURE 6

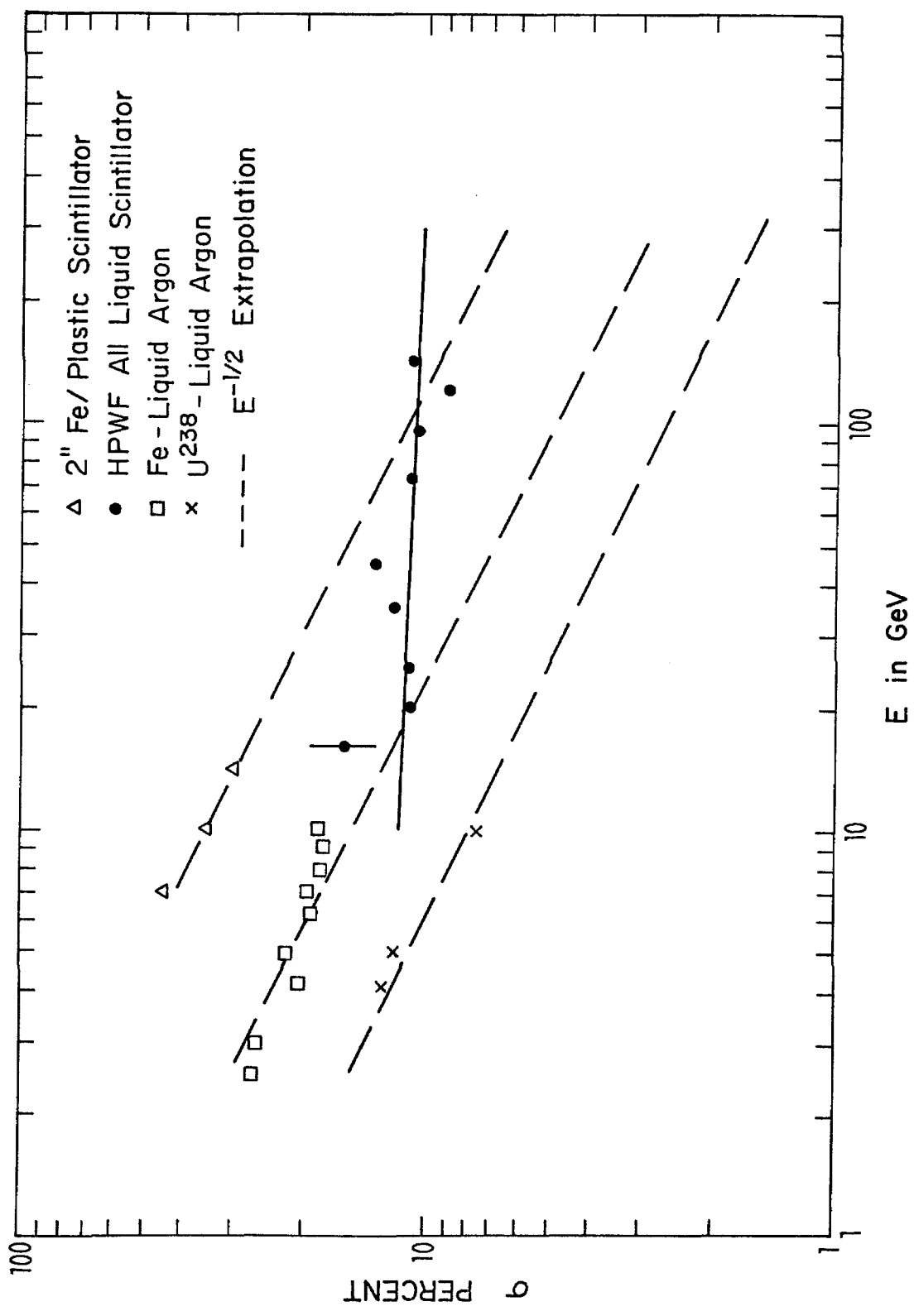


FIG. 7 RESOLUTION VS. ENERGY

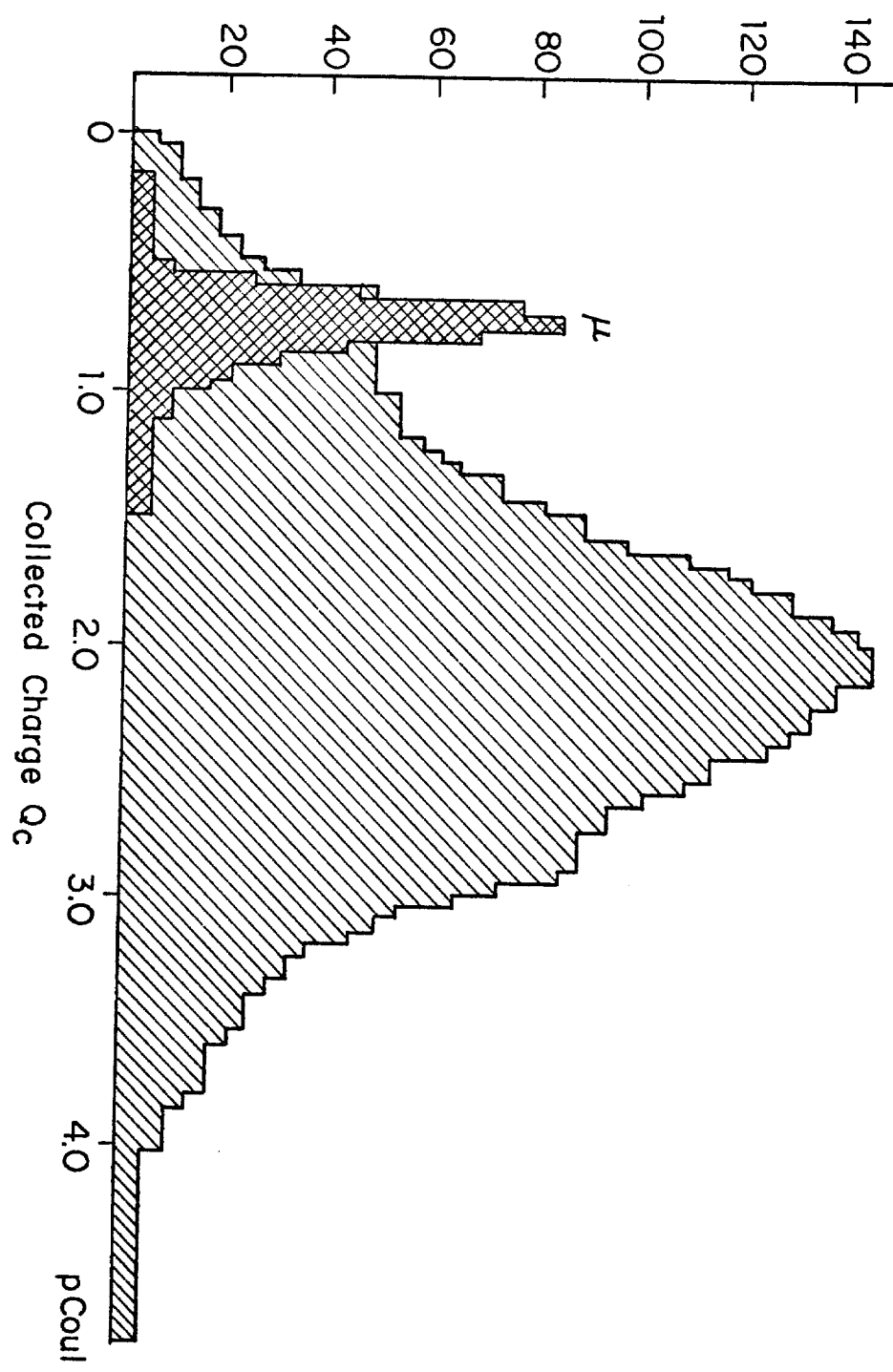
vs energy for Fe/plastic, Fe/liquid argon, and U²³⁸/liquid argon. Iron/liquid argon is still superior in energy resolution to Fe/plastic, again by a factor of two or so.

Resolution in x and y

A SLAC/LBL group²⁶ has measured the position of a shower produced by 4 GeV/c electrons incident on a lead/liquid argon calorimeter to 2 mm using 2 cm samplings across the face of the shower and five samplings along its length. Measurements with a 10 GeV/c pion beam incident on an iron/liquid argon calorimeter have been made at CERN.^{20,27} These measurements, although much more crude than the SLAC/LBL studies, indicate that at least 2 cm resolution on the centroid of the charge distribution for hadron showers can be achieved, if the sampling is fine grained enough.

This group also indicates that single muons can be distinguished easily from hadrons as is shown in Figures 8 and 9 taken from reference 22. Figure 8 shows the collected charge for 10 GeV/c π^- and μ^- gotten by demanding that the region around a "track" contain less than 4 times the amount of charge deposited by a minimum ionizing particle. In Figure 9 this criteria has been strengthened by demanding that this associated charge be less than 1 times minimum ionizing: it is claimed that no muons are lost by making this cut. These measurements indicate that it is possible to track a single minimizing particle through the calorimeter; we will then have essentially 100% acceptance for muons from charged current interactions. This should reduce the contamination of these events in our neutral current sample to a negligible amount.

Recent measurements at CERN³² indicate that, at 22 GeV, a resolution of $\sigma(\theta_H) = 30$ mrad can be achieved. Measurements at lower energies indicate that the formula



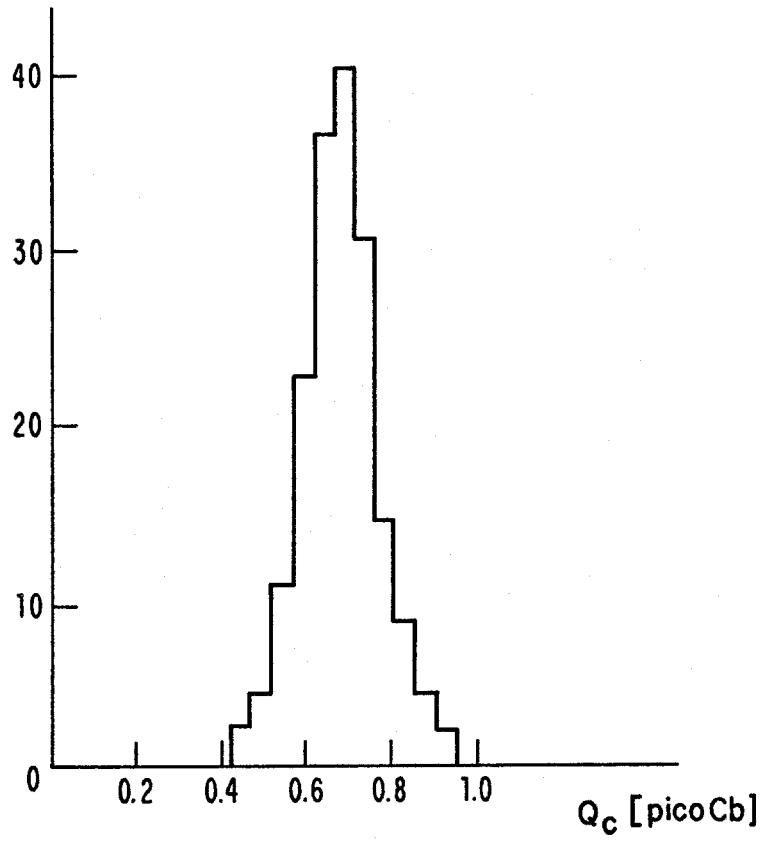


FIGURE 9

MUON SIGNAL OBTAINED BY MORE RESTRICTIVE CONDITIONS; EFFICIENCY IS UNCHANGED.

$$\sigma(\theta_H) = 0.004 + \frac{0.60 \text{ GeV}}{E_H}$$

is a good representation of the data. This implies $\sigma(\theta_H) = 10$ mrad at 100 GeV. With the geometry we propose, which is similar in sampling frequency to the test calorimeter used at CERN, we expect similar angular resolution.

Using the proposed geometry we have calculated, using Monte Carlo methods, the resolution in $x = Q^2/2m_p \nu$ in the following way. Monte Carlo data were generated according to the distribution $\alpha(1-x)^3$. The data were then passed through the apparatus with appropriate resolutions and a fit was made to the result. This is shown in Figure 10 for a sample of only 2000 events; we take $E_\nu = 260 \text{ GeV} \pm 9\%$, $E_{\text{Hadron}} > 150 \text{ GeV}$, $\sigma_{E \text{ Hadron}} = 0.75/\sqrt{E_h}$ and $\sigma(\theta_H) = 10$ mrad. The $\sigma(\theta_H)$ is a pessimistic estimate at these energies. Fitting to the analyzed distribution a function of the form $A(1-x)^N + C$ we get $N = 2.77 \pm 0.17$, to be compared with the input distribution of $N = 3$. The agreement is good.

We have calculated, via Monte Carlo, the ability of the detector to measure the difference between a flat distribution in y and $f(y) = (1-y)^2$. We have taken a worse case

$$\sigma_{E \text{ Hadron}} = 0.75/\sqrt{E_H}$$

$$\sigma(\theta_H) = 10 \text{ mrad},$$

and neutrino energies gaussian distributed around $E_\nu = 260 \text{ GeV}$ with a $\sigma = 9\%$ which is what we expect for a given neutrino energy. We have fit to the function $f(y) = C + A(1-y)^2$ for an experiment of 500 events. The results are given in the following table.

$$f(y) = C + A(1 - y)^2: 0.2 \leq y \leq 0.9$$

<u>A</u>	<u>C</u>	<u>A</u> <u>A + C</u>	<u>Analyzed A + C for 500 Events</u>
0	1	0	0.09 ± 0.23
1/2	1	0.5	0.40 ± 0.18
1	1	0.5	0.52 ± 0.16
1	0.5	0.67	0.66 ± 0.15
1	0	1	1.03 ± 0.06

This indicates that in a 2,000 event experiment, in most regions of x, y and E_ν , good measurements of A can be made.

B. HPWF Muon Spectrometer

We envisage using the HPWF muon spectrometer with the present spark chambers replaced by drift chambers. We feel that the noise generated by the present optical chambers will be intolerable considering the sensitive electronics demanded by the calorimeter. Drift chambers of the appropriate size have been built at Harvard and may be made available for use with this facility. If they are not we plan to build the needed chambers.

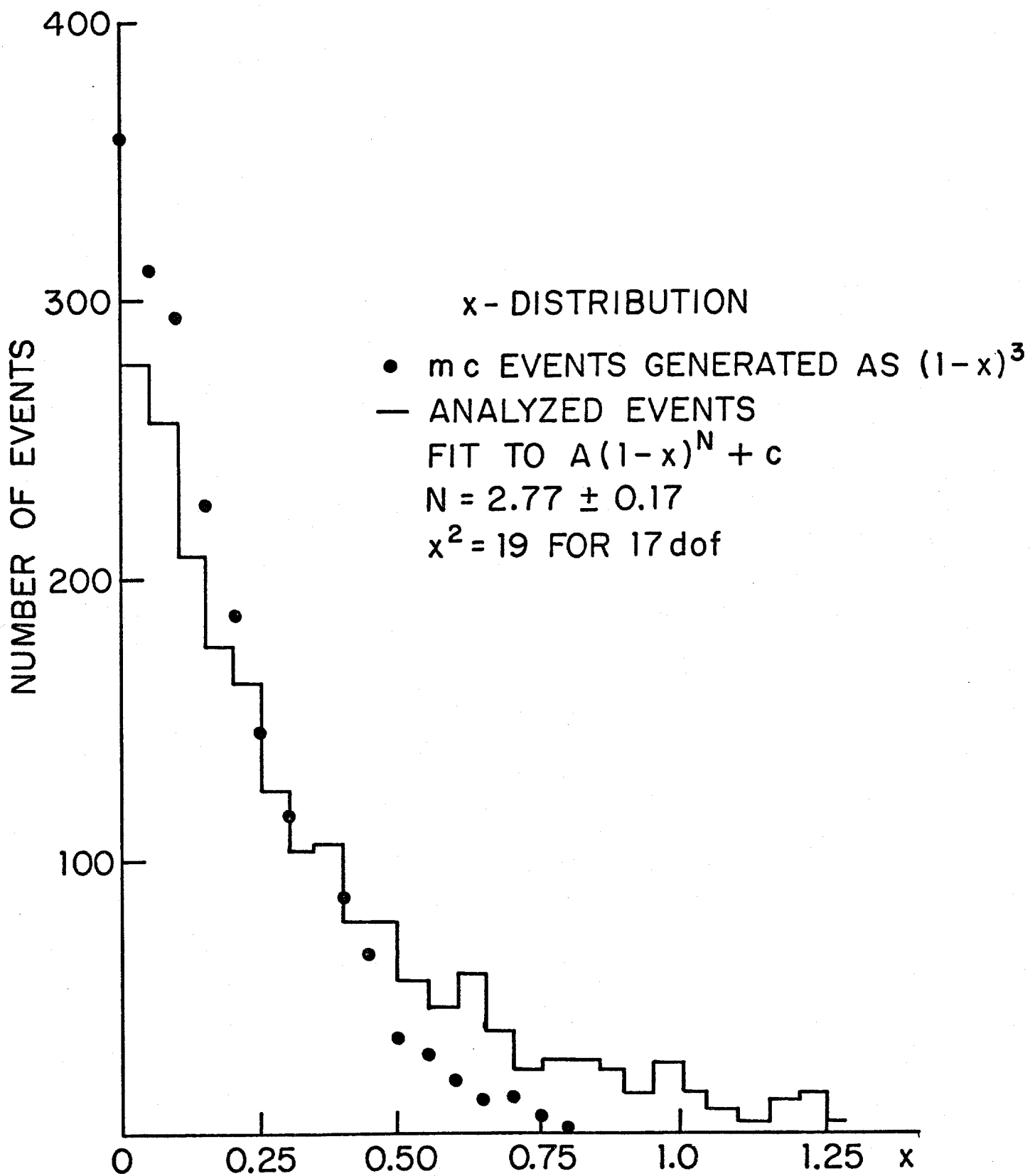


FIGURE 10

IV. The Beam and Event Rates

The final size of the fiducial volume was determined by our desire to make high statistics measurements of neutral current phenomena over a large kinematic region, using the dichromatic beam that is presently being built at Fermilab.⁴ The calculated spectra of neutrinos and antineutrinos expected from this beam are shown in Figures 11 and 12 respectively.

In order to have a large y coverage, which demands a good knowledge of the incoming neutrino momentum, it is necessary to situate the detector away from zero degrees with respect to the beam line. This fact is illustrated in Figure 13. Here we have plotted neutrino energy against lab angle. The first thing to note is that the neutrinos from pion decay are all concentrated at less than 1 mrad from zero degrees while the neutrinos from k -decay extend beyond 5 mrad. The second fact is that the region from 1 to 3 mrad contains neutrinos in the range $70 \text{ GeV} < E_\nu < 210 \text{ GeV}$. The neutrino energy is known, from the angle of the neutrino, which means the position of the interaction across the face of the detector, to an accuracy defined by the momentum resolution of primary K -meson beam, $\pm 9\%$. There is essentially no background from π -neutrinos! A detector that subtends ± 1 mrad centered at 2 mrad with respect to the nominal beam line would cover the entire y range; energy deposition cuts which severely limit the y range accessible to study unnecessary.

We have calculated the event rate expected in the proposed detector situated at 2 mrad with a fiducial volume of $3 \text{ m} \times 3 \text{ m} \times 12 \text{ m}$ which is $4090 \text{ gms/cm}^2 \times 9 \text{ m}^2$ of target. The results are given in Tables 3 and 4 for neutrinos and antineutrinos, where we have taken into account the loss in solid angle. We note that the number of events per day, roughly 100, is less by a factor of about 60 than

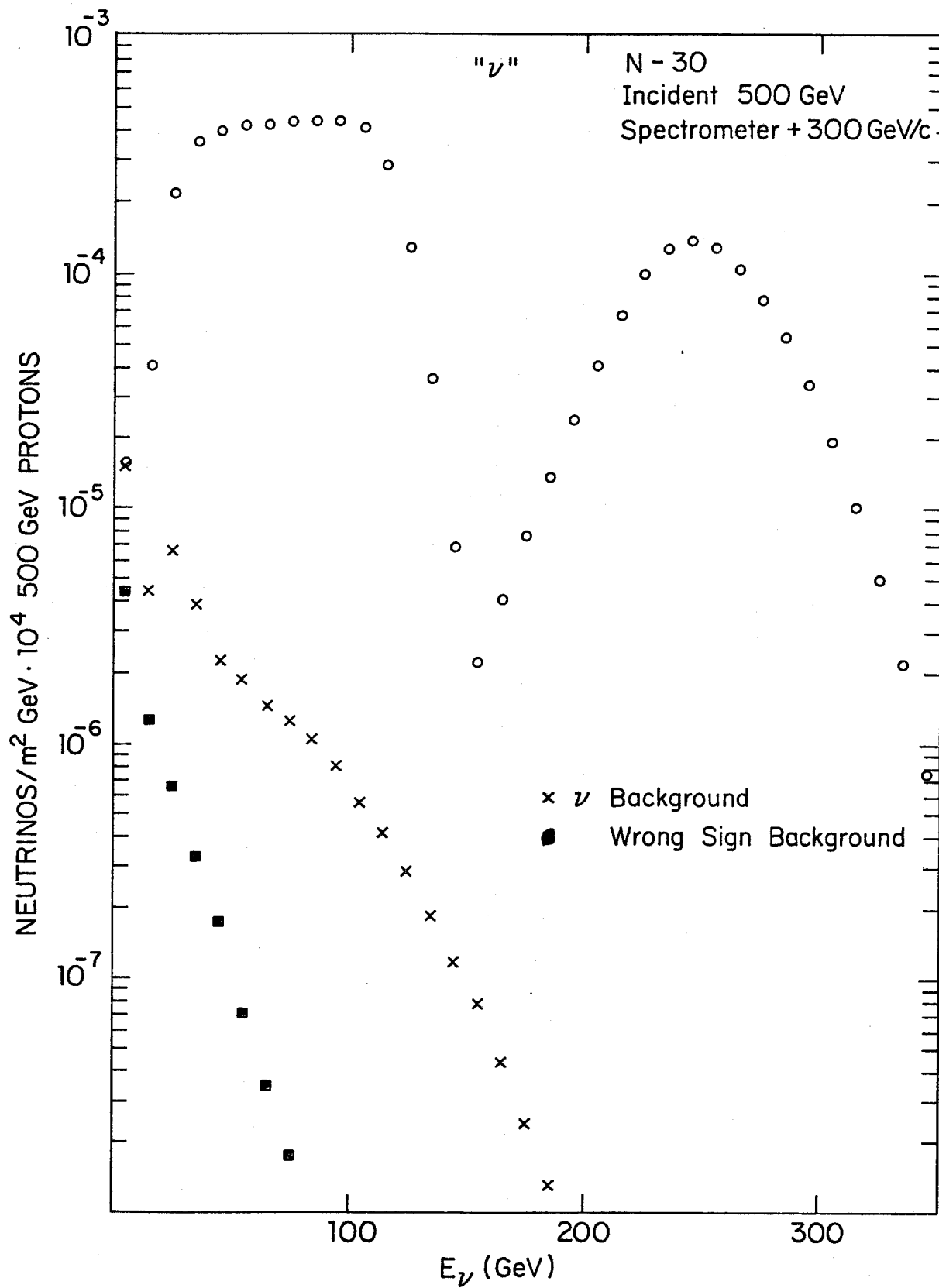


FIGURE 11

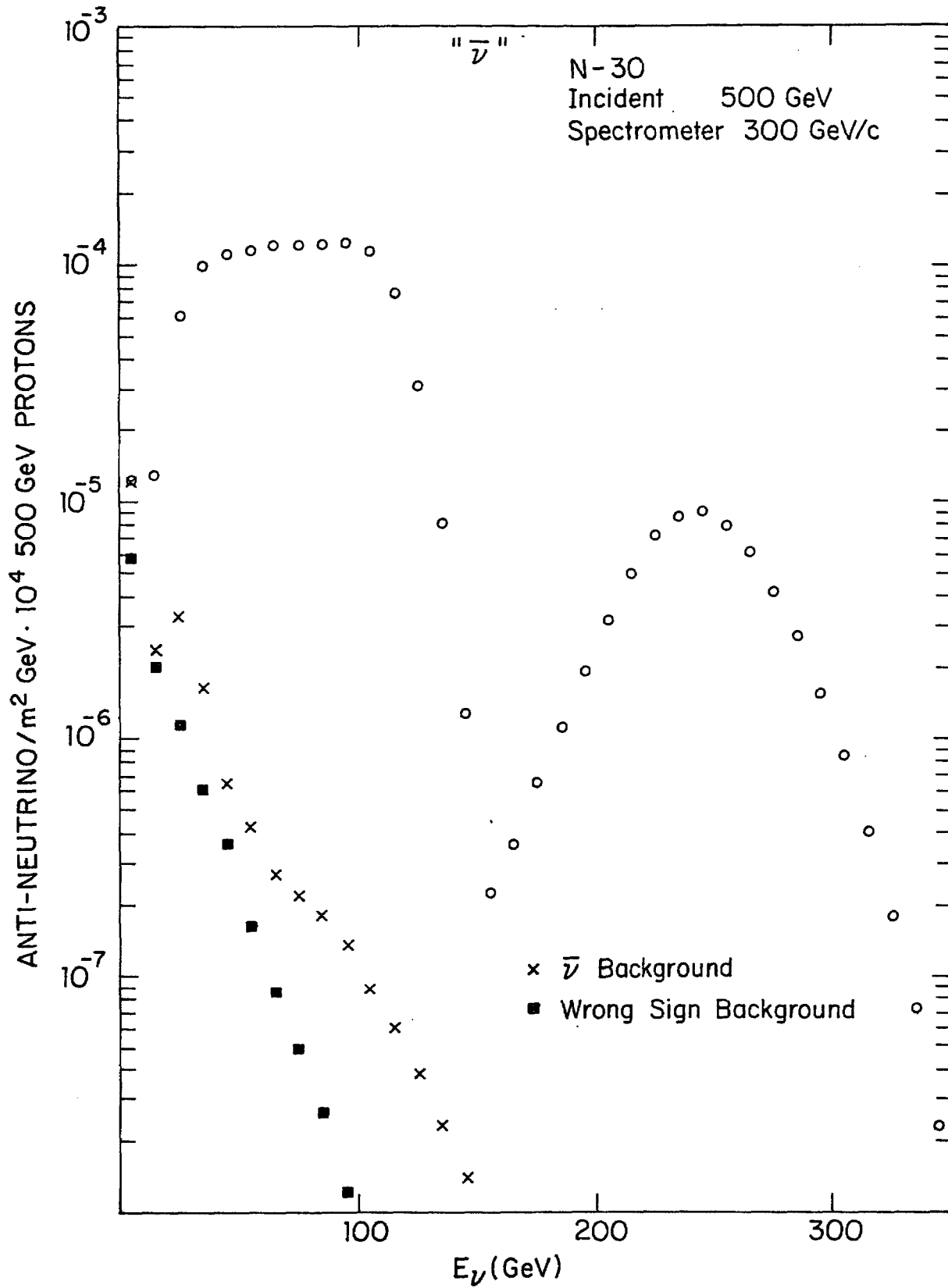


FIGURE 12

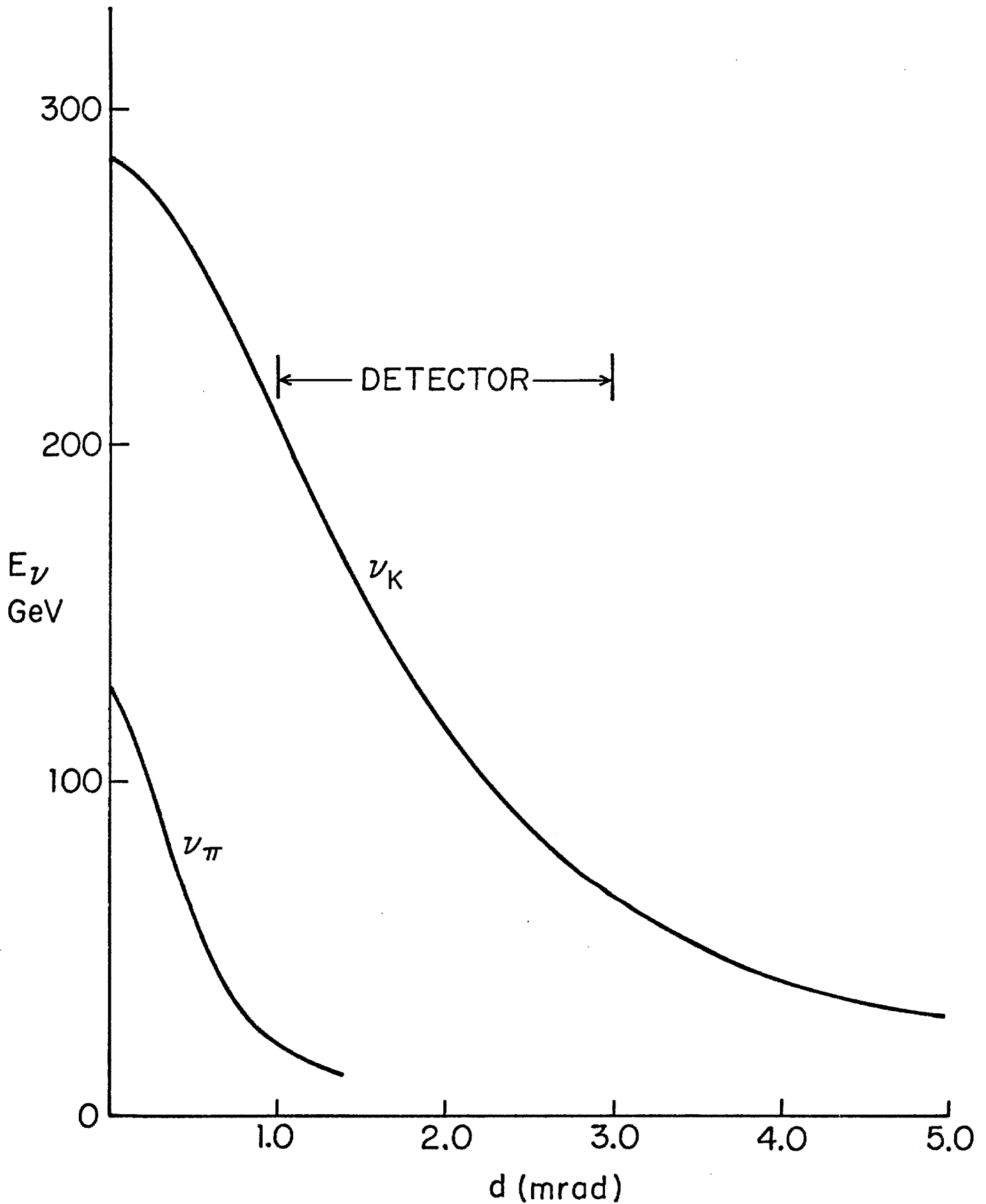


FIG. 13 E_ν VS DECAY ANGLE IN THE LAB FOR
E PRIMARY = 300 GeV

Table 3Event Rate - Neutrinos

$$\left(\sigma^{\nu} = 0.83 E_{\nu} \times 10^{-38} \text{ cm}^2\right)^1$$

<u>E_ν (GeV)</u>	<u># Events per 10¹³ Protons on Target</u>
70	9.53 × 10 ⁻⁷
80	1.96 × 10 ⁻⁶
90	3.99 × 10 ⁻⁶
100	7.84 × 10 ⁻⁶
110	1.65 × 10 ⁻⁵
120	2.86 × 10 ⁻⁵
130	5.30 × 10 ⁻⁵
140	9.54 × 10 ⁻⁵
150	1.84 × 10 ⁻⁴
160	3.71 × 10 ⁻⁴
170	6.95 × 10 ⁻⁴
180	1.23 × 10 ⁻³
190	2.33 × 10 ⁻³
200	4.03 × 10 ⁻³
210	7.44 × 10 ⁻³
	<u>Total: 0.0165/10¹³ protons</u>

100 Events/Day

Day ≡ 5 pulses/min × 20 hrs.

Table 4Event Rate - Antineutrinos

$$\left(\sigma_{\bar{\nu}} = 0.28 E_{\nu} \times 10^{-38} \text{ cm}^2\right)^1$$

<u>$E_{\bar{\nu}}$ (GeV)</u>	<u># Events per 10^{13} Protons on Target</u>
70	-----
80	-----
90	-----
100	2.99×10^{-7}
110	5.06×10^{-7}
120	9.65×10^{-7}
130	1.79×10^{-6}
140	3.22×10^{-6}
150	5.86×10^{-6}
160	1.10×10^{-5}
170	1.95×10^{-5}
180	3.72×10^{-5}
190	6.55×10^{-5}
200	1.06×10^{-4}
210	1.93×10^{-3}
	<u>$2.18 \times 10^{-3} / 10^{13}$ protons</u>

13 events/day

what one would get at zero degrees. However, if we are to study the details of neutral currents we must know the incoming neutrino energy; moving away from zero degrees seems the best way of accomplishing this goal. This fact indicates that bubble chambers are not suitable for this kind of study because the event rates would be prohibitively low.

Since we plan to build the calorimeter in a way that facilitates moving it, we can optimize its position for the largest flux with an acceptably low contamination from pion neutrinos.

V. Comparison with CERN SPS

	<u>This Proposal</u>	<u>WA 1*</u>	<u>WA 18⁺</u>
Useful Target	4089 gms/cm ²	8558	2200
E _h -Resolution (σ)	50% E ^{-1/2}	90% E ^{-1/2}	55% E ^{-1/2}
X-Resolution	20 - 30%	None	20 - 30%
Beam	Dichromatic N-30 Beam	Dichromatic and wide band	Dichromatic
Cost	\$1.4 × 10 ⁶	-----	-----
Completion	~2 years after approval	Data taking	Fall 1978
Goals	ν, ν̄ neutral currents; W ² structure in cross sections; comparisons with charged currents with very good resolution in x and y; anomalous events in neutral currents	-----	-----

* Steinberger

+ Winter P 49

VI. Preliminary Cost Estimate

1. Dewar	\$100K ^a	
2. Plumbing	30K ^b	
3. Air pads	40K ^c	
4. Electronics	600K ^d	
5. Steel plates and steel strips	350K ^e	
6. Drift chambers	(100K) ^f	
7. Computer	(40K) ^g	
8. Liquid argon storage and supply	(60K) ^h	
9. Trigger counters	50K ⁱ	
10. Contingency (20%)	<u>229K</u>	
Total:	\$1399K	(\$1599K)

Assembly: 5 men × 1 year

- a. Engineering estimate for a double walled carbon and stainless steel dewar. Includes internal G-10 support structure.
- b. Includes oxygen monitoring devices. Does not include microprocessor.
- c. Engineering estimate for 900 ton support system.

- d. Cost of 30,000 channels of electronics, microprocessor and cables. Assumes the use of hybrid integrated circuits and the multiplexing of 1000 channels of sample and hold electronics per ADC. Design work in progress.
- e. Approximately 471 tons of ready to use (smooth and punched) steel plate, 1.5 mm thick, at a cost of \$744/ton. This may go down to \$500-\$600/ton.
- f. Drift chambers of the size required already exist. It is hoped that they can be acquired for the muon spectrometer. If not the cost will be approximately \$10K per chamber.
- g. A computer of appropriate size and speed (PDP 11/45 or PDP 15) can be acquired without new expenditures.
- h. This includes liquid nitrogen and liquid argon storage and transfer pipes. We assume that this will be supplied by Fermilab. This does not include the cost of argon or nitrogen which we also hope Fermilab will provide.
- i. Trigger counters will be placed inside the calorimeter in 5 places along its length. The counters are 2 feet \times 6 feet in a 2 \times 6 array. We assume \$300/square meter for scintillator, \$200 per phototube and \$50 for shield and base. This comes to \$7800/plane.

VII. Summary

We propose to carry out a high statistics study of the interaction of neutrinos with matter. To do this we propose to build a liquid argon-iron hadron calorimeter to be used in conjunction with the HPWF muon spectrometer with the spark chambers replaced by drift chambers. The device we propose is uniquely suited to study neutral current reactions; it is also an excellent tool for the study of charged currents.

References

1. B. Roe, "New Results in High Energy Neutrino Physics," invited talk presented at the APS, DPF meeting at BNL, October 1976.
2. A. Benvenuti, et al., Phys. Rev. Lett. 37, 1095 (1976).
3. A. De Rujula, "Quark Tasting with Neutrinos," to be published in the proceedings of the 1976 Coral Gables Conference, Miami, January 1976.
4. D. Edwards, S. Mori and S. Press, "350 GeV/c Dichromatic Neutrino Target Train," Fermilab TM-661, 2972.000, May 6, 1976; D. A. Edwards and F. J. Sciulli, "A Second Generation Narrow Band Neutrino Beam," Fermilab TM-660, 2972.000, May 1976.
5. A. Pais and S. B. Treiman, Phys. Rev. Lett. 35, 1556 (1975).
6. F. J. Sciulli, CALTECH Preprint 68-520, October 1975.
7. See L. Wolfenstein, "Theory of Neutral Currents and Anomalous Neutrino Interactions," invited talk presented at the International Symposium on Lepton and Photon Interactions at High Energies, Stanford, August 1975, and references therein.
8. B. C. Barish, et al., 1975 Neutrino Conference, Paris.
9. E. A. Paschos and V. A. Zacharov. Phys. Rev. D8, 215 (1973).
10. A. De Rujula and S. L. Glashow, Phys. Rev. D9, 180 (1973).
11. D. H. Perkins, Contemporary Physics 16, 174 (1975).
12. B. Aubert, et al., Phys. Rev. Lett. 33, 984 (1974).
13. A. Benvenuti, et al., Phys. Rev. Lett. 36, 1478 (1976).
14. B. C. Barish, et al., 1976 Neutrino Conference, Aachen.
15. A. Benvenuti, et al., Phys. Rev. Lett. 34, 597 (1975).
16. B. C. Barish, in proceedings of the 6th Topical Conference in Particle Physics, Honolulu, 1975.
17. J. Heim, "Engineering Design and Analysis of Large Superconducting Particle Analysis Magnets," Fermilab TM-522, 2750.000, October 3, 1974; "Superconducting Magnet Systems at Fermilab," Fermilab TM-591, July 1975.
18. J. Heim, private communication.

19. E. S. Sadowski, private communication.
20. C. W. Fabjan, et al., "Iron Liquid Argon and Uranium Liquid Argon Calorimeters for Hadron Energy Measurement," CERN preprint, September 1976.
21. T. A. Gabriel and K. Chandler, Particle Accelerators 5, 161 (1973); Nucl. Instr. and Meth. 116, 333 (1974); T. A. Gabriel and J. D. Amburgey, "Calibration Calculations of Hadronic Cascades Induced by High Energy Muons in Iron/Plastic Calorimeters," ORNL/TM-5615 December 1976; see also: T. A. Gabriel, "A Computational Approach to Ionization Spectrometer Design," Proc. of Calorimeter Workshop, Batavia, May 1975.
22. L. R. Sulak in Proc. of Calorimeter Workshop, Batavia, May 1975.
23. W. A. Gibson, et al., in ORNL-3940, May 1966, pg. 110.
24. Fast Neutron Physics, J. B. Marion and J. L. Fowler, eds., Interscience, New York, 1960.
25. M. Holder, et al., "Proposal to Study High Energy Neutrino Interactions at the SPS," CERN/SPSC/P 73-1, 27 July 1973; SPSC/P 73-1/Add. 8 January 1974; Experiments at CERN in 1976, CERN Grey Report, October 1976.
26. D. Hitlin, et al., SLAC Pub. 1761, May 1976.
27. CERN-Hamburg-Karlsruhe-Oxford-Rutherford Laboratory-Westfield College Collaboration CERN/SPSC/4-98/M3, October 4, 1974.
28. M. F. James, AEEW-M863 (1969); W. H. Walker, AECL-3109 (1968).
29. T. A. Gabriel and W. Schmidt, "Calculated Performances of Iron-Argon and Iron-Plastic Calorimeters for Incident Hadrons with Energies of 5 to 75 GeV," ORNL/TM-5105, February 1976.
30. T. A. Gabriel, private communication.
31. J. Steinberger, presented at SPSC Meeting, March 5, 1977.
32. R. S. Orr, private communication.
33. J. D. Bjorken, "Weak Interaction Theory and Neutral Currents," SLAC Pub 1866, January 1977.
34. E. Fischback, J. Gruenwald, S. Rosen and B. Kayser, PRL 37, 582 (1976); B. Kayser, G. Garvey, E. Fischback and S. Rosen, Phys. Lett. B 52, 385 (1974).
35. J. Pati and A. Salam, Phys. Rev. D 8, 1240 (1973).
36. R. N. Mohapatru, J. C. Pati and B. P. Sidhu, Univ. of Maryland Preprint No. 77-102.

ADDENDUM TO P-541,
"A PROPOSAL TO STUDY NEUTRAL CURRENT NEUTRINO AND ANTINEUTRINO INTERACTIONS"

B. Eisenstein, L. Holloway
University of Illinois at Urbana-Champaign

A. L. Sessoms, C. Tao, R. Wilson
Harvard University

S. C. Wright
University of Chicago

SPOKESMAN:

A. L. Sessoms
High Energy Physics Laboratory
42 Oxford Street
Cambridge, Massachusetts 02138
617-495-5889
(FTS 830-5889)

In this addendum we indicate minor changes in our calorimeter design based on prototype studies. We also indicate a change in proposed running posture that permits us to take the full beam without losing significantly in our knowledge of the neutrino energy or in our kinematic coverage. Event rates for this configuration are given.

Calculations indicate that it is essential that the calorimeter be placed in front of the 24 foot muon spectrometer in Lab C. These calculations are discussed in detail in the appendix.

I. Target/Calorimeter

The target/calorimeter parameters are given in Table 1. The minor changes come from detailed studies of the plate and strip support structure. In this configuration, with 3 mm thick plates and a 4 mm deep argon gap, 5 x strips and 5 y strips are ganged together to give coordinate measurements every 3/4 interaction length. This gives an average of 10 x, y points per shower, which is more than adequate to measure its direction. The sampling is fine enough so that fluctuations are not a problem.

II. Position

Detailed calculations, which are described in the Appendix, indicate that, of the iron muon spectrometers in existence at Fermilab, only the 24 foot muon spectrometer in Lab C gives coverage enough to allow a background free sample of neutral current events to be taken. These calculations indicate that 98.5% of the charge current events are rejected; a cut of $y \leq 0.9$ increases this to over 99%. The detector position with respect to the beam is shown in Figure 1. Clearly a wider range in energy coverage can be attained by changing the beam direction.

III. Event Rate

The event rate has been calculated in the following way. Taking the N-30 beam spectrum given in the proposal the number of events as a function of energy are calculated. Cuts are then imposed on y such that the hadron energy is greater than the pion neutrino corresponding to that position in the detector. The results are given in Table 2. We get approximately 1600 neutrino induced events per day. Of these approximately 320 are due to the neutral current interaction.

Table 1Target Calorimeter

Active Dimensions	$3.8 \times 3.8 \text{ m}^2$
Length	11.7 m
Sampling Step	3.0 mm iron (2.36 gm/cm^2)
Sampling Counter (Energy)	Liquid argon, 4 mm thick, iron plates $3.8 \times 3.8 \text{ m}^2$
Sampling Counter (Angle)	Liquid argon, 4 mm thick, iron plates $3.8 \text{ m} \times 0.02 \text{ m}$ x and y, every 28 mm
Modularity	209 modules of 4, $3.6 \times 3.6 \text{ m}^2 \times 3.0 \text{ mm}$ plates and 2 sets of $3.6 \times 0.02 \text{ m}^2 \times 3.0 \text{ mm}$ x and y strips
Total Quantities	Target weight 404 tons Target thickness 4089 gms/cm^2 Total weight 870 tons 30,000 channels of electronics
Average Quantities	Density $\rho = 4.17 \text{ gms/cm}^3$ Radiation length: 3.52 cm Interaction length: 19.0 cm
Performance	<u>Vertex Resolution</u> $\sigma = 0.6 \text{ cm}$ <u>Shower Direction</u> $\sigma(\theta_H) = 0.004 + \frac{0.6(\text{GeV})}{E_H}$ or $\pm 10 \text{ mrad}$ at 100 GeV <u>Hadron Energy Resolution</u> $\frac{\sigma(E_H)}{E_H} = \frac{0.5}{\sqrt{E(H)}}$

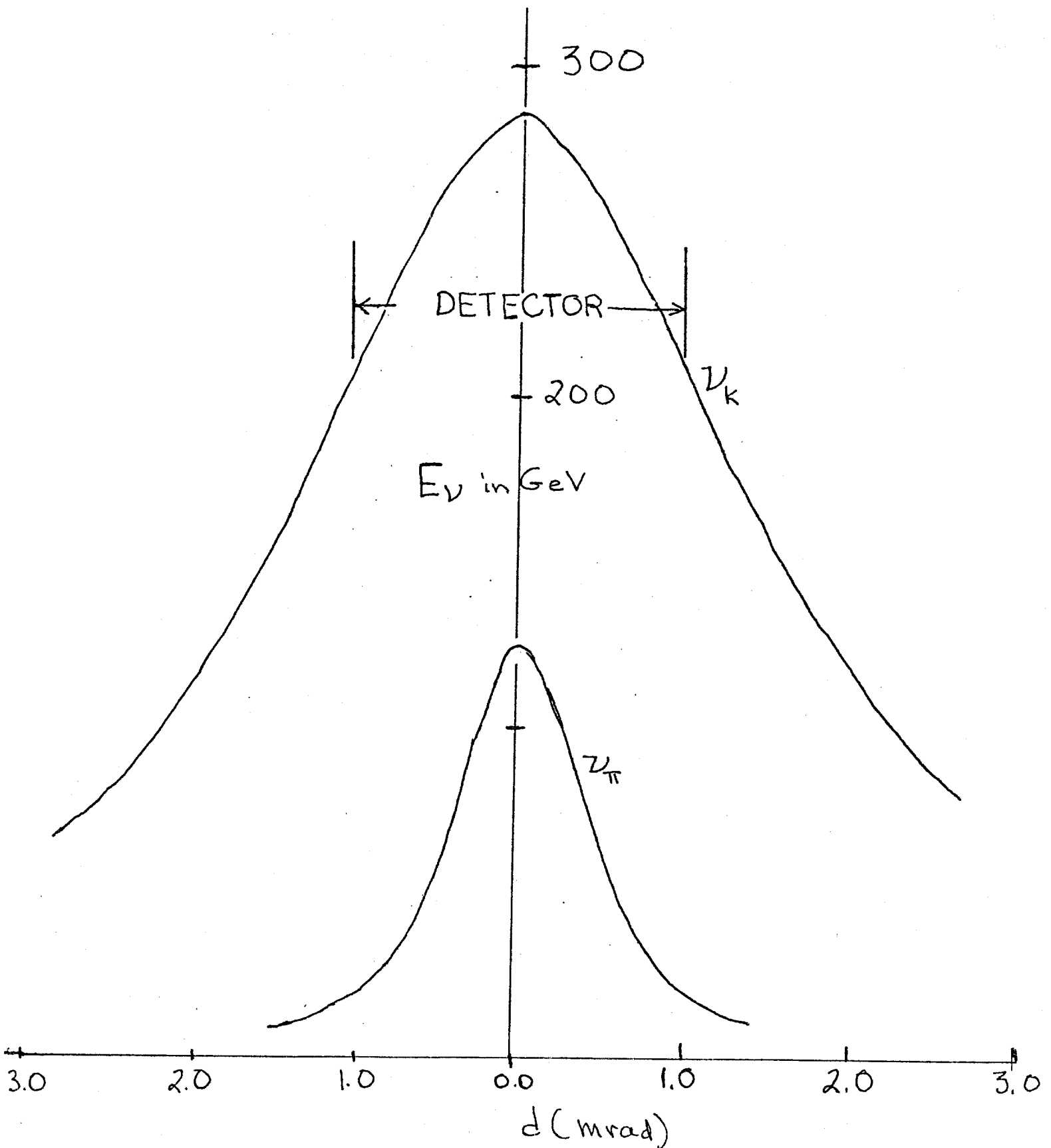


Figure 1. E_ν VS DECAY ANGLE IN THE LAB FOR
E PRIMARY = 300 GeV

Table 2

Event Rate - Neutrinos

$$(\sigma^{\nu} = 0.83 E_{\nu} \times 10^{-38} \text{ cm}^2)$$

<u>E (GeV)</u>	<u># Events per 10¹³ Protons on Target</u>
175	37 × 10 ⁻⁴
200	195 × 10 ⁻⁴
225	633 × 10 ⁻⁴
250	977 × 10 ⁻⁴
275	613 × 10 ⁻⁴
300	215 × 10 ⁻⁴
325	<u>46 × 10⁻⁴</u>
	Total 0.272/10 ¹³ protons

1630 Events/Day

Day ≡ 5 pulses/min × 20 hours

APPENDIX

Monte Carlo Simulation of Experiment

CONTENTS:

- A. Brief Description of Method
- B. Summary of Important Parameters
- C. Some Results on Resolution of Measured Quantities
- D. Study of Charged Current Background in Neutral Current Data Sample

A. Brief Description of Method

1) Generation

A beam kaon is chosen from a given distribution and is allowed to decay in the decay pipe. The neutrino is tracked to the calorimeter fiducial volume and is allowed to interact within it with a probability proportional to both E_ν and the path length within the fiducial volume.

Values of x and y are chosen for the produced hadron from given distributions. This then fixes all kinematic quantities for the event. The hadron is then oriented (randomly) in azimuth about the neutrino direction, thereby fixing the event in space.

2) Measurement

Gaussian errors are folded into:

the hadron energy

the projected angles of the hadron direction

the coordinates of the interaction point.

A "measured" neutrino direction is constructed by joining the interaction point with the midpoint of the decay pipe. A "measured" E_ν is calculated by assuming the decay of an on-axis kaon whose momentum is the central value of the input distribution. [The neutrino energy is also calculated for the case of a pion decay. The event is accepted only if its measured hadron energy is larger than the pion-parent neutrino energy, assuring an unambiguous determination of E_ν .]

From the measured neutrino, and the measured hadron energy and angles, all other kinematic quantities are calculated.

3) Outgoing Lepton

The real and measured outgoing lepton, assumed here to be a muon, is tracked out of the calorimeter and through (if its energy is sufficient) a downstream muon identifier. Neutral current event candidates are those whose measured lepton would be detected downstream if it were a muon, and whose real lepton is not detected downstream. Real leptons are not detected downstream if the event is a neutral current event (good data) or if it is a charged current event with either a wide-angle or low-energy muon ("charged current background"). The final event sample thus consists of both neutral current and background charged current events.

B. Summary of Important Parameters

Meson beam: gaussian about $p_0 = 250$ GeV/c with $\sigma = 22.5$ GeV/c (9% momentum bite)

Meson direction: gaussian about 0° with $\sigma = .22$ mrad

Meson position transverse to beam line: gaussian with $\sigma = 5$ cm

Hadron energy measurement: gaussian with $\sigma/E_h = .5/\sqrt{E_h}$ (GeV)

Projected angles of hadron: gaussian with $\sigma = .004 + .6/E_h$ (GeV)
(10 mrad at 100 GeV)

Error on interaction point: gaussian with $\sigma = 1$ cm

Calorimeter located in Lab C

Fiducial volume $3.2 \times 3.2 \times 9.8 \text{ m}^3$

Muon identifier: 24' diam \times 2.0 m

x distribution: $(1 - x)^3$

y distribution: $0.76 + 0.24 (1 - y)^2$

C. Some Results on Resolution of Measured Quantities

From the "measuring" procedure described in Appendix A2 it is clear that only E_h (measured) is expected to be gaussian distributed about E_h with a sigma that is specified. For all other measured quantities, Q_m , whose true value is Q , we anticipate that $\langle Q_m - Q \rangle \neq 0$. To study this the Monte Carlo events, generated with standard parameters from Appendix B, were divided into intervals of each measured quantity Q_m , and $\langle Q \rangle$ was plotted versus $\langle Q_m \rangle$ in each interval. The interval of Q_m is indicated by the horizontal error bars on each point, and the RMS (or σ) of $Q_m - Q$ by the vertical error bars.

Figure C1 shows the neutrino energy. There is little systematic shift, and $\sigma/E_\nu \sim 9\%$, the momentum bite of the meson beam.

The error on y is shown in Figure C2. Again, there is little systematic shift. The error on y, σ_y , varies roughly linearly with y, being $\sim .025$ at $\langle y_m \rangle = .15$ and $\sim .075$ at $\langle y_m \rangle = .75$.

The hadron mass error is shown in Figure C3. There is a significant (2σ) difference between $\langle m_h \rangle$ and $\langle m_h \text{ (measured)} \rangle$ at $\langle m_h \text{ (measured)} \rangle = 6 \text{ GeV}$

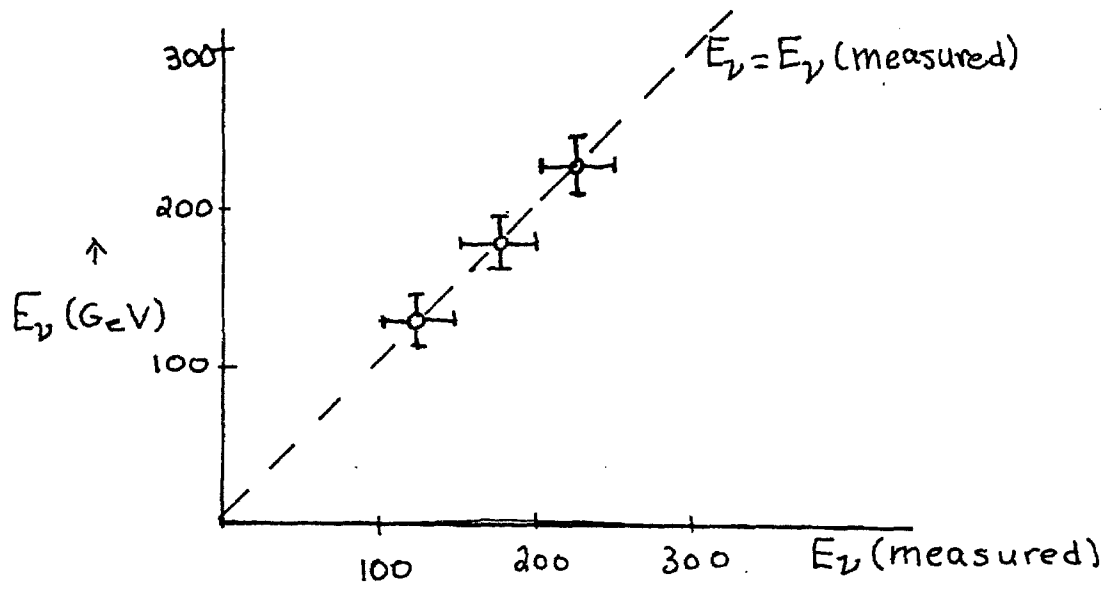


figure C1

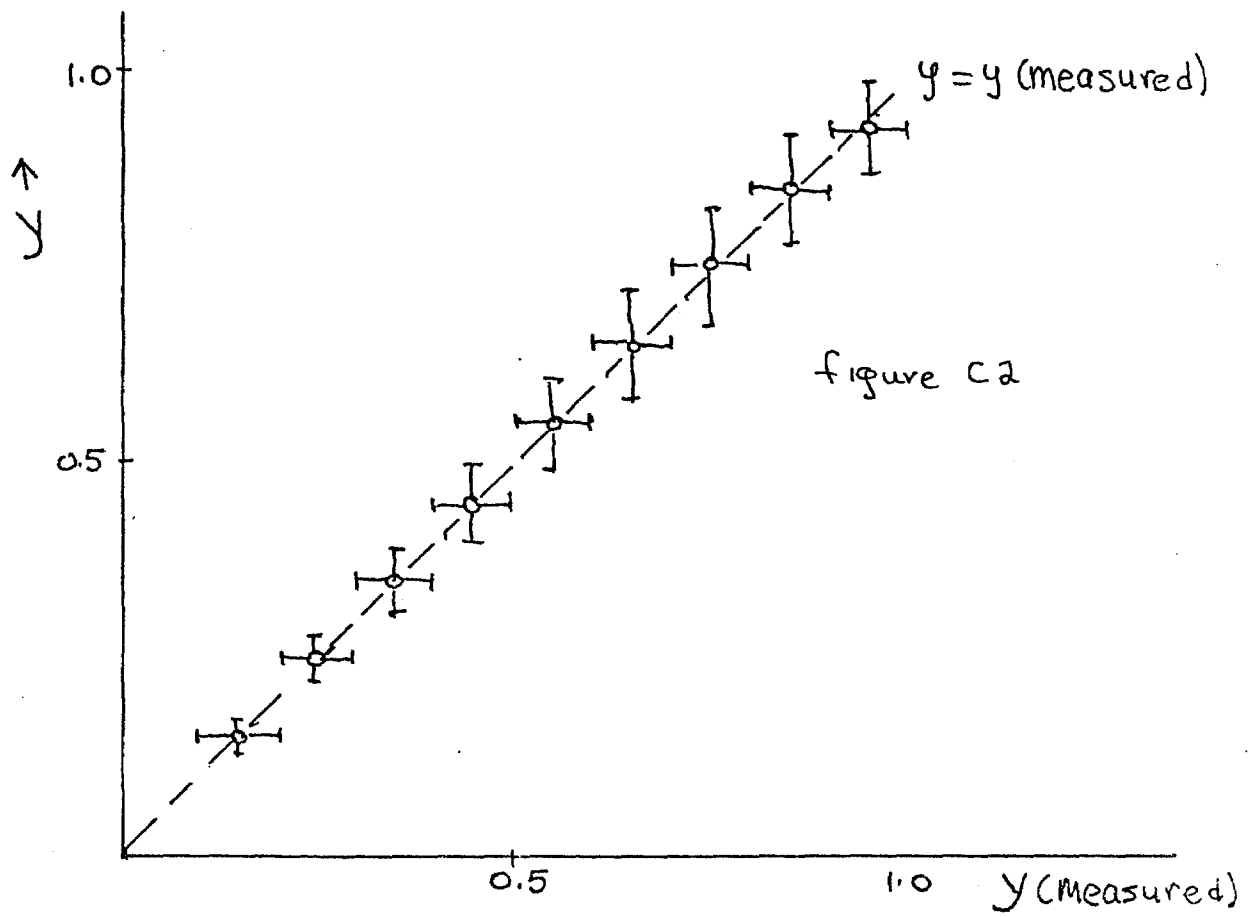


figure C2

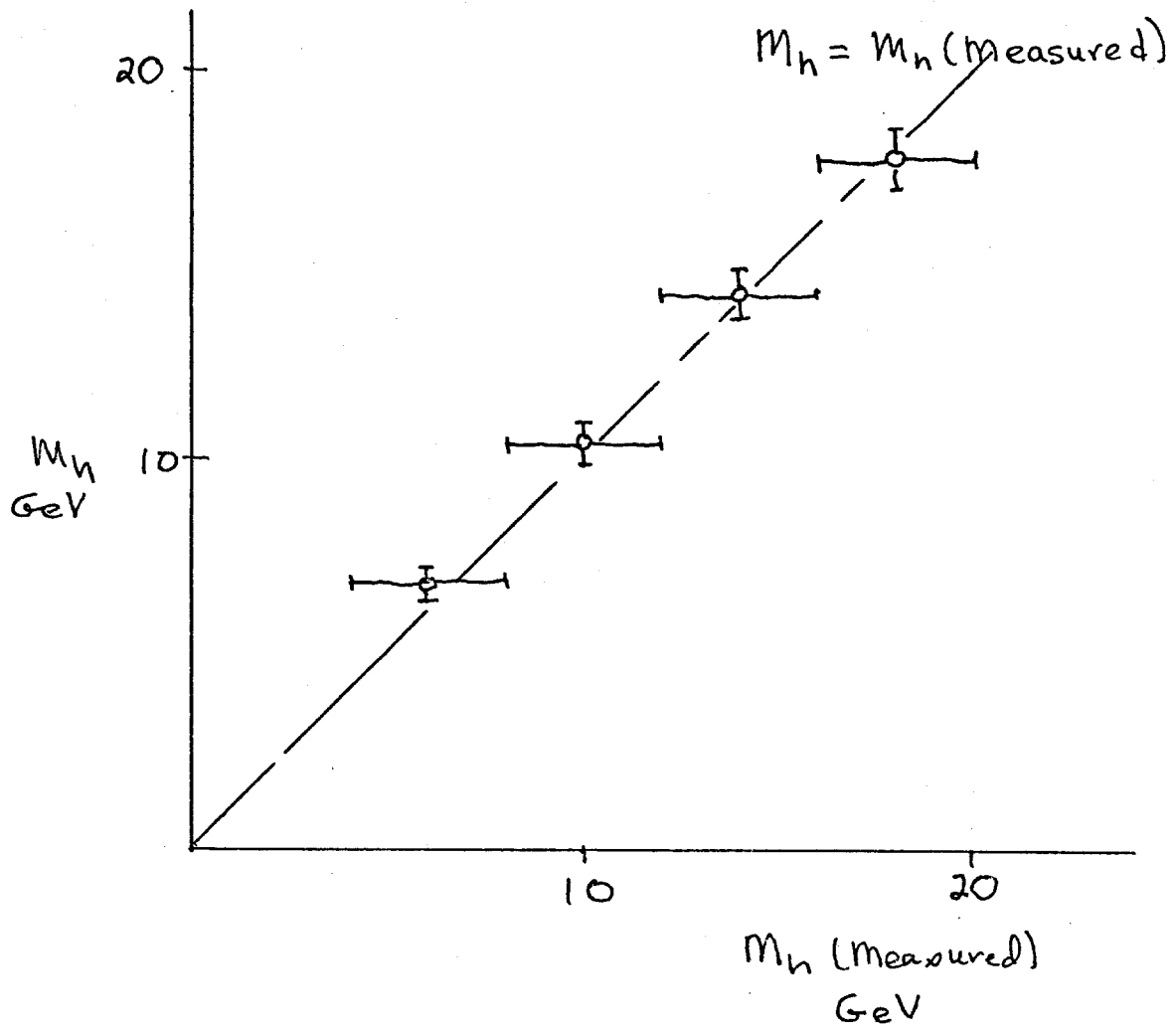


figure C3

but the shift decreases as m_h increases. The error σ increases, roughly linearly, from ~ 0.4 GeV at 6 GeV to ~ 0.7 GeV at a $\langle m_h \rangle$ of 18 GeV.

x versus $x(\text{measured})$ is shown in Figure C4a. A large systematic shift occurs for $x \sim 0.5$, but we anticipate that most of the data will occur at smaller x . Shown separately in C4b is the vertical error bar, σ_x , versus $x(\text{measured})$. As a consistency check, σ_x was hand-calculated using the following simplifying assumptions:

y fixed at $\langle y \rangle \sim 0.5$

E_ν fixed at $\langle E_\nu \rangle \sim 200$ GeV

E_h fixed at $\langle E_h \rangle \sim 100$ GeV

[hadron angle error fixed at 10 mrad (appropriate to $E_h = 100$ GeV)]

The result of the calculation is shown as the curve in Figure C4b.

Its general agreement with the Monte Carlo data at $x \sim 0.5$ (where most of the Monte Carlo events are found) is a reassuring consistency check.

D. Charged Current Background in Neutral Current Data Sample

Following the procedure described in Appendix A, especially section 3, an experiment was performed with 2000 neutral current interactions and 8000 charged current interactions in the calorimeter. The same x and y distributions were used for both. Of the neutral current events, 1823 were kept as good data by virtue of the fact that their outgoing measured leptons, had they been muons, would have penetrated 2 meters of a 24' diameter downstream muon identifier. The y distribution for these events is shown in Figure D1.

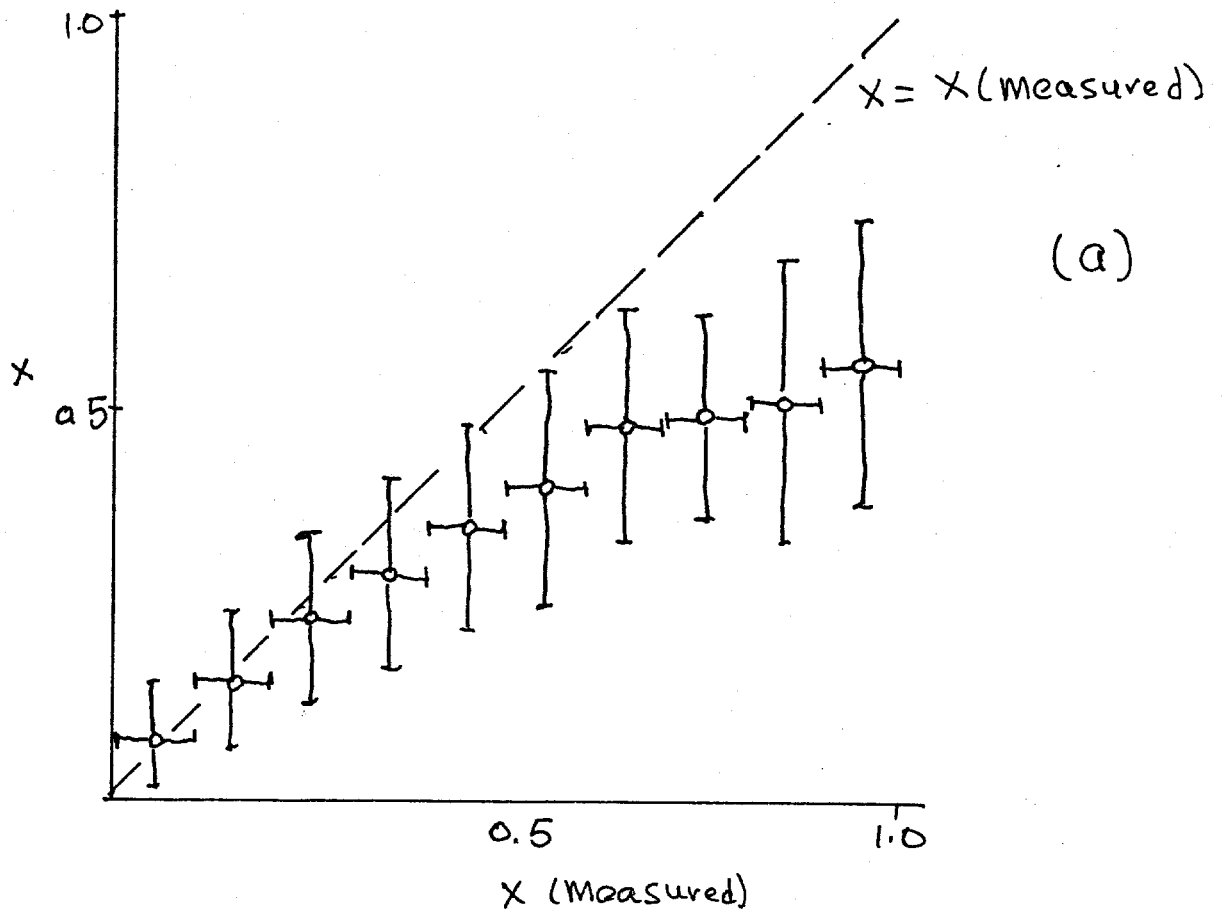
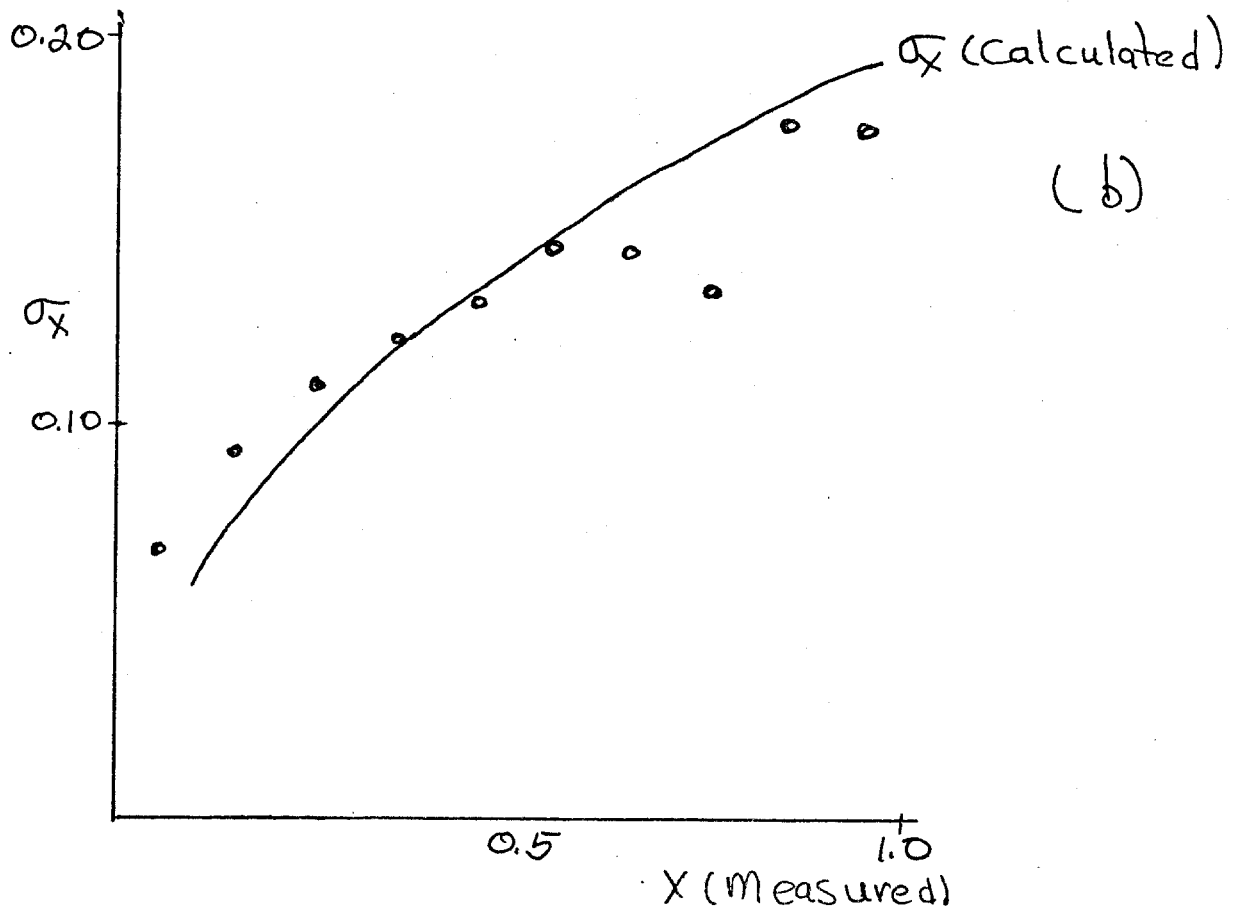


figure C4

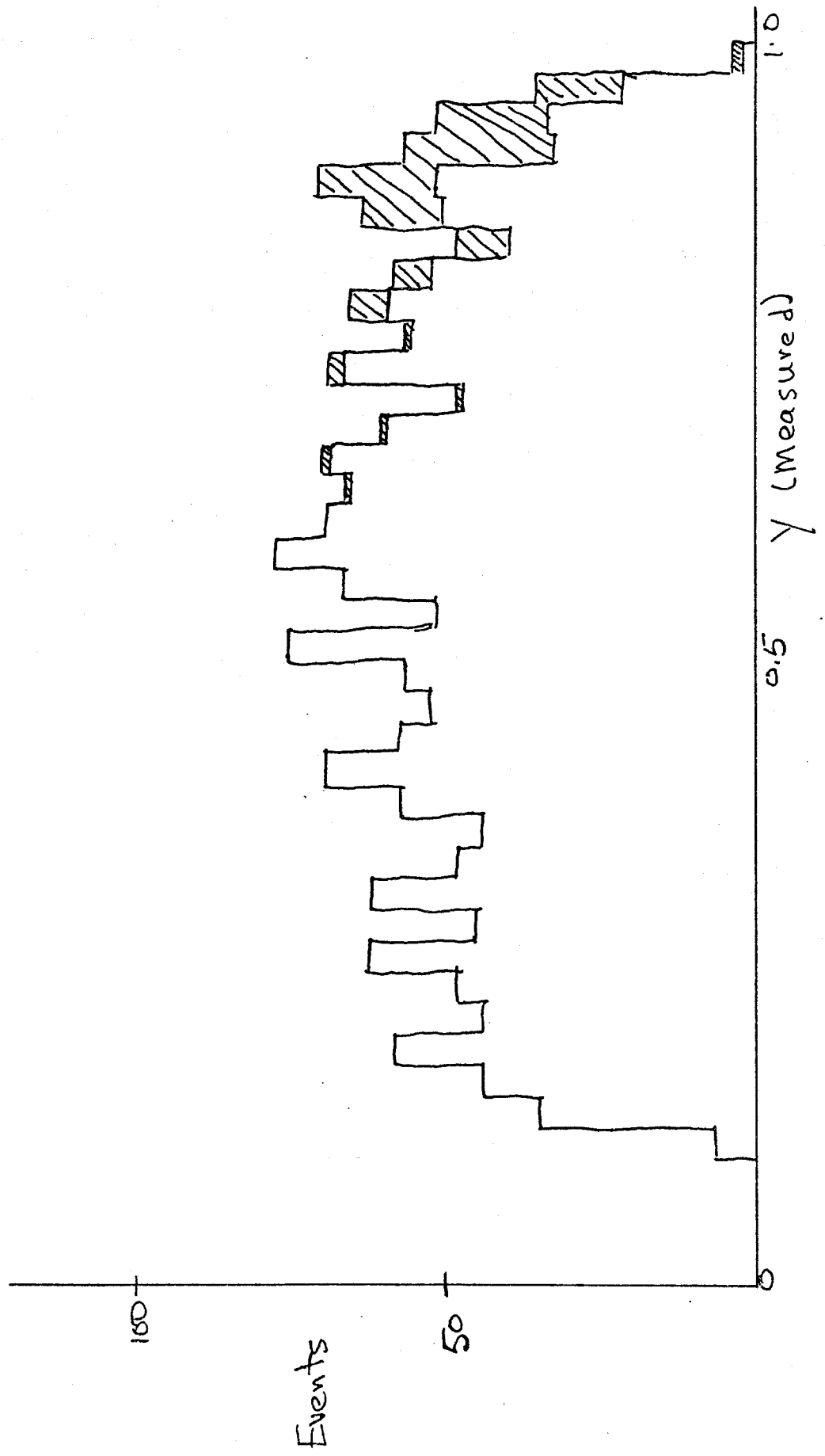


1823 events from 2000 Neutral Current events in the calorimeter
Shaded: 118 charged current bkgd. from 8000 CC events

figure D.1

24 foot Muon Spectrometer

$$\frac{\text{Bkgd}}{\text{Signal}} = 6.5\%$$



Of the charged current events, 118 had measured muons that penetrated the identifier, but whose actual muons did not. These events became background added to the neutral current good data. They are characterized by having $y \approx 1$, and are shown shaded in Figure D1. The background is significant for $y \gtrsim 0.85$.

The experiment was repeated for a 12' diameter muon identifier, and the results are shown in Figure D2. Now only 1525 neutral current events remain as good data, and 314 charged current events are included as background. The background is significant for $y \gtrsim 0.7$, and the total background/signal ratio is 20.6% compared to 6.5% for the 24' diameter identifier.

1525 events from 2000 Neutral Current events in the calorimeter
shaded: 314 charged current bkgd. from 8000 cc events

figure D2

12 foot Muon Spectrometer

$$\frac{\text{Bkgd}}{\text{Signal}} = 20.6\%$$

